Research Square

Preprints are preliminary reports that have not undergone peer review.
They should not be considered conclusive, used to inform clinical practice,
or referenced by the media as validated information.

Functional heterogeneity among four co-occurring landfill bacteria during low-density polyethylene transformation

Sandeep Kumar

sandeepkumar@ddu.du.ac.in

Deen Dayal Upadhyaya College University of Delhi

Alisha Srivastwa

Deen Dayal Upadhyaya College University of Delhi

Sweta Singh

IMS University Courses Campus

Harshita Singh

Deen Dayal Upadhyaya College University of Delhi

Syed Ali Abbas

Chandigarh University

Ravinder Singh

Chandigarh University

Research Article

Keywords: Low-density polyethylene, Plastic-associated bacteria, Dyella japonica, Pantoea agglomerans, Biofilm, FTIR spectroscopy

Posted Date: October 30th, 2026

DOI: https://doi.org/10.21203/rs.3.rs-11237907/v1

License: This work is licensed under a Creative Commons Attribution 4.0 International License.
Read Full License

Additional Declarations: No competing interests reported.

Functional heterogeneity among four co-occurring landfill bacteria during low-density polyethylene transformation

Sandeep Kumar[1*], Alisha Srivastwa[1], Sweta Singh[2], Harshita Singh[1], Syed Ali Abbas[3] and Ravinder Singh[3]

[1] Department of Botany, Deen Dayal Upadhyaya College, University of Delhi, New Delhi, Delhi 110078, India

[2] Department of Biotechnology, IMS University Courses Campus, Ghaziabad (NCR), Uttar Pradesh 201015, India

[3] Department of Biotechnology, Chandigarh University, Gharuan, Mohali, Punjab 140413, India

[*]**Corresponding author:** Sandeep Kumar, sandeepkumar@ddu.du.ac.in

ORCID: Sandeep Kumar- https://orcid.org/0000-0002-2757-4093

Acknowledgements

The authors thank Prof. Hem Chand Jain, Principal, Deen Dayal Upadhyaya College, University of Delhi, New Delhi, India, and Prof. Sachchidanand Tripathi, Teacher-in-Charge, Department of Botany, Deen Dayal Upadhyaya College, University of Delhi, for laboratory facilities and for fostering an environment conducive to the smooth functioning of the department.

Abstract
Low-density polyethylene (LDPE) transformation is usually reported for individual isolates, whereas direct comparisons among co-occurring bacteria from the same contaminated habitat are scarce. Four Gram-negative bacteria were isolated from a plastic-contaminated municipal dumpsite in Ghaziabad, India, and identified by 16S rRNA gene sequencing as *Pseudomonas* sp. DW, *Dyella japonica* DP, *Enterobacter* sp. DLY and *Pantoea agglomerans* DY. Growth, extracellular enzyme profiles, gravimetric loss, microscopy, scanning electron microscopy (SEM) and Fourier transform infrared (FTIR) spectroscopy were compared over 45 days under a common framework. All isolates grew best at 30 °C and pH 7.0. *Pseudomonas* sp. DW showed the highest apparent mass loss (16.07 ± 0.18%), carbonyl index (0.2444) and hydroxyl index (0.1773), the most extensive biofilm, and the only lipase/esterase activity under nutrient limitation. *Enterobacter* sp. DLY lost 13.96 ± 0.14% of mass and had a carbonyl index of 0.2031 without detectable lipase/esterase activity. To our knowledge, *D. japonica* DP and *P. agglomerans* DY are the first isolates of these species characterised for LDPE transformation at species level; only genus-level reports exist for *Dyella* and *Pantoea*, and *Pseudomonas* and *Enterobacter* are established LDPE-associated genera, so no taxonomic novelty is claimed for them. The principal novelty is the within-site comparison showing that similar endpoints can arise from different trait combinations, which guides strain selection for mechanistic and consortium studies.

Keywords Low-density polyethylene, Plastic-associated bacteria, *Dyella japonica*, *Pantoea agglomerans*, Biofilm · FTIR spectroscopy

1. Introduction

Plastics are synthetic, petroleum-derived polymers whose low cost, durability, and versatility have made them indispensable across nearly every sector of modern life (Thompson et al. 2009; Charnock 2021). Yet the same molecular features that confer this utility high molecular weight, hydrophobic and chemically inert backbones, and crystalline domains render plastic waste highly resistant to natural degradation (Wilkes and Aristilde 2017). Global plastic production has risen from roughly 1.3 million tonnes in 1950 to approximately 460 million tonnes in 2019, a 230-fold increase, and is projected to nearly triple by 2060 in the absence of intervention (OECD 2022; Cai et al. 2023). Of this volume, only 9-10% is recycled globally, while the remainder is landfilled, incinerated, or leaked into rivers and oceans an estimated 109 million tonnes into riverine systems and 30 million tonnes into marine environments in 2019 alone (OECD 2022). The consequences extend well beyond accumulation, plastic's full life cycle currently generates approximately 1.8 gigatonnes of CO_2-equivalent emissions annually (OECD 2022), while progressive fragmentation into microplastics and nano-plastics degrades soil structure, disrupts microbial communities, and introduces endocrine-disrupting plasticizers such as phthalates into food chains (Kotova et al. 2021; Cai et al. 2023; Dhali et al. 2024).

The scale of the problem is especially acute in rapidly urbanising economies where waste-management infrastructure has not kept pace with plastic consumption. India, among the largest plastic-waste generators globally (NITI Aayog 2022; EY India 2025), illustrates this: official estimates suggest that only around 60% of its plastic waste is formally collected, leaving a substantial fraction to enter the environment as unmanaged waste (NITI Aayog 2022). National policy analyses have accordingly called for accelerated development of biodegradable alternatives and microbially mediated degradation technologies for recalcitrant polyolefins such as polyethylene and polypropylene, alongside strengthened Extended Producer Responsibility frameworks (NITI Aayog 2022). This reflects a broader recognition, not confined to any one country, that conventional management routes landfilling, incineration, and mechanical recycling are structurally insufficient to address the scale of the problem, given the land pressure, toxic emissions, and poor economic viability associated with each (Alshehrei 2017; Bakht et al. 2020).

Microbial bioremediation has consequently emerged as one of the most promising sustainable alternatives. Bacteria and fungi colonize plastic surfaces to form biofilm communities the "plastisphere" that mediate degradation through sequential attachment, bio-fragmentation, assimilation, and mineralization, driven by

extracellular hydrolytic enzymes such as esterases, lipases, and cutinases (Urbanek et al. 2018; Dhali et al. 2024). Bacterial genera including *Pseudomonas*, *Bacillus*, *Enterobacter*, and *Ideonella* have demonstrated degradative activity across major polymer classes, including polyethylene, polystyrene, and polyethylene terephthalate (Yoshida et al. 2016; Skariyachan et al. 2021; Isha et al. 2024). Indigenous strains isolated directly from plastic-contaminated sites often outperform laboratory reference strains owing to prolonged in-situ adaptation (Maroof et al. 2021; Tirkey and Upadhyay 2025).

Recent studies reinforce the value of landfill-derived microorganisms but also show that the field is moving beyond isolate discovery alone. Individual strains have now been reported with low-density polyethylene (LDPE) transformation supported by weight loss, Fourier transform infrared spectroscopy (FTIR) and scanning electron microscopy (SEM), while mixed cultures and landfill enrichments have been investigated for improved degradation and community-level function. These studies make simple claims of 'a new LDPE-associated bacterium' increasingly difficult to distinguish from incremental strain screening. The unresolved question addressed here is narrower and more comparative: when several LDPE-associated isolates are recovered from the same landfill habitat and exposed to the same polymer under the same culture conditions, do differences in apparent mass-loss magnitude correspond to differences in measurable biochemical and surface-associated traits? In particular, we asked whether lipase/esterase induction, biofilm architecture and FTIR-detected oxidation covary across isolates, or whether substantial LDPE-associated mass loss can occur without detectable esterolytic activity. This framing deliberately treats the enzyme assays, SEM and FTIR as complementary phenotypic evidence rather than as direct identification of a complete transformation pathway. We therefore hypothesized that co-occurring isolates would show distinct combinations of enzyme expression, surface colonization and polymer oxidation even when their overall ability to reduce LDPE mass was broadly similar. To test this, four indigenous isolates from one plastic-contaminated landfill were characterized side-by-side using identical physiological, biochemical, gravimetric, microscopic and spectroscopic assays. The study does not test a mixed consortium directly; instead, it provides a comparative basis for selecting and subsequently testing strains with potentially complementary phenotypes.

The taxa examined here differ in how much is known about their LDPE-associated behaviour. *Pseudomonas* and *Enterobacter* are well-established LDPE-associated genera, including in India (Sarker et al. 2020; Shilpa et al. 2024; Sharma and Neelam 2025), and *Pantoea* has been reported at genus level in LDPE studies (Skariyachan et al. 2016; de Fretes et al. 2024). *Dyella* sp. has, to our knowledge, been detected only within mixed microplastic-degrading assemblages (Ren and Ni 2023). To our knowledge, no species-level LDPE data exist for *Dyella japonica* or *Pantoea agglomerans*, and neither species has been compared with *Pseudomonas* and *Enterobacter* isolates from the same habitat. This study is therefore framed as a within-site comparative report in which *D. japonica* DP and *P. agglomerans* DY are, to our knowledge, characterised for LDPE transformation for the first time, while *Pseudomonas* sp. DW and *Enterobacter* sp. DLY provide benchmarks from well-studied genera.

2. Materials and methods

2.1 Study site, sample collection, and isolation of indigenous bacteria

Study site and rationale. Soil sampling was conducted at an open municipal dumping site located at AH2, Kanawani Village, Indirapuram, Ghaziabad, Uttar Pradesh, India (28.636° N, 77.392° E). The site was selected on the basis of its sustained and visible accumulation of mixed plastic waste, including polyethylene carry bags, multilayer food-packaging material, and other domestic solid waste, much of which showed evidence of long-term environmental weathering surface embrittlement, discoloration, and partial fragmentation attributable to prolonged exposure to sunlight, humidity, and mechanical abrasion. Such weathering is known to increase plastic surface roughness and microporosity, thereby enhancing microbial attachment and colonization (Wei and Zimmermann 2017). Dumpsites of this nature impose chronic selective pressure on the resident soil microbiota, favouring the persistence of bacterial populations that have acclimatized to utilize plastic polymers and their breakdown products as alternative carbon sources. Comparable plastic-contaminated environments have

previously yielded plastic-associated genera such as *Pseudomonas*, *Bacillus*, *Micrococcus*, and *Staphylococcus* (Javid et al. 2024), supporting the suitability of this site for isolating candidate degrader strains.

Sample collection. Soil samples were collected from the surface horizon (0-15 cm), the depth at which aerobic microbial density is typically greatest, using a sterile stainless-steel trowel after removal of loose surface debris and stones. Approximately 200-300 g of soil was collected per sampling point and transferred into sterile, pre-labelled, airtight containers. All sampling implements were surface-decontaminated with 70% ethanol between collections to avoid cross-contamination. Samples were transported to the laboratory under cold-chain conditions (~4°C) and processed within 24 h of collection to preserve indigenous microbial viability and minimize population shifts prior to isolation.

Isolation of bacterial strains. Bacterial isolation was carried out using the standard serial dilution and spread-plate technique. One gram of soil was suspended in 50 mL of sterile distilled water and agitated to obtain a homogeneous suspension, which was then serially diluted up to 10^{-6} in sterile distilled water. Aliquots (0.1 mL) of the higher dilutions (10^{-4}-10^{-6}) were spread onto Luria-Bertani (LB) agar plates under aseptic conditions within a laminar airflow chamber (Dubey and Thalla 2025) and incubated at 37°C for 24-48 h. Following incubation, colonies differing in size, shape, pigmentation, and margin characteristics were selected and subjected to repeated streak-plating on fresh LB agar until morphologically and microscopically uniform, axenic cultures were obtained. Purified isolates were maintained on LB and LB Agar slants and stored at 4°C for short-term use, with glycerol stocks prepared for longer-term preservation.

2.2 Phenotypic screening and physiological characterization

Screening for plastic-associated growth. Purified isolates were screened in Minimal Salt Medium (MSM), a nutrient-limited medium used to reduce growth supported by readily available organic carbon (Ali et al. 2021). In solid assays, sterilized LDPE film was placed on MSM agar and inoculated cultures were monitored for growth and colonization. In liquid assays, UV-treated LDPE pieces (2 × 2 cm) were introduced into MSM broth inoculated with each isolate and culture turbidity was monitored. Isolates showing reproducible growth in the LDPE-containing condition were selected for further characterization. Because growth in a minimal medium can be affected by residual inoculum-derived nutrients, these assays were interpreted as evidence of plastic-associated growth potential rather than as stand-alone proof of LDPE carbon assimilation.

Morphological characterization. Selected bacterial isolates were morphologically characterized by Gram staining to determine their Gram reaction, cell shape, and cellular arrangement following standard microbiological procedures (Tripathi et al. 2025). A thin bacterial smear was prepared on a clean glass slide, heat-fixed, and subjected to the Gram staining procedure using crystal violet, Gram's iodine, alcohol decolorization, and safranin as the counterstain. The stained preparations were examined under a bright-field light microscope using a 100× oil immersion objective (total magnification, 1000×). The Gram reaction (Gram-positive or Gram-negative), cell morphology (cocci, bacilli, or other forms), and cellular arrangement were recorded for each isolate and used as preliminary phenotypic characteristics for bacterial identification.

Optimization of physiological growth parameters. To identify the conditions most conducive to isolate growth and, by extension, to plastic transformation activity, shortlisted isolates were subjected to a systematic optimization of three physicochemical variables: incubation temperature (20°C, 25°C, 30°C, and 35°C), medium pH (5, 6, 7, and 8), and nutrient availability (comparing growth in nutrient-rich LB medium against nutrient-limited MSM). In each case, bacterial growth was quantified spectrophotometrically by measuring optical density at 610 nm (OD_{610}) following a standardized incubation period, allowing direct comparison of growth response across treatment levels. This step was undertaken because microbial degradation efficiency is strongly influenced by the prevailing physicochemical environment, and identifying isolate-specific optima is a prerequisite for designing effective downstream degradation assays and, ultimately, for translating laboratory findings into field-applicable bioremediation protocols.

Biosafety-associated phenotypic screening. Because the isolates were being considered for possible environmental bioremediation research, they were screened for selected phenotypic markers relevant to biosafety. The panel comprised Indole, Methyl Red (MR), Voges-Proskauer (VP), Simmons' citrate utilization, deoxyribonuclease (DNase) and blood-agar haemolysis assays, performed according to established protocols (MacFaddin 2000; Chioma et al. 2013; Haas et al. 2014; Bochalya et al. 2016; Lad et al. 2022). Antibiotic susceptibility was also assessed against cefepime, penicillin, chloramphenicol, neomycin and streptomycin by disc diffusion on Mueller–Hinton agar (Al-Ajeeli 2024). These assays were used to describe virulence-associated phenotypes and antimicrobial susceptibility; they were not treated as a definitive determination of pathogenicity or environmental safety, particularly for taxa that may contain opportunistic pathogens.

Enzymatic profiling. To characterize extracellular enzymatic phenotypes potentially relevant to polymer-surface transformation, isolates were further screened for the production of extracellular hydrolytic enzymes with established relevance to plastic transformation. Catalase activity was assessed by the hydrogen-peroxide bubble test; cellulase, esterase/lipase, α-amylase, and protease activities were assessed using substrate-specific agar plate assays (carboxymethyl-cellulose, tributyrin, starch, and skim-milk agar, respectively), with the formation of clear zones around bacterial colonies following appropriate developer treatment where applicable taken as evidence of positive enzymatic activity (Charnock 2021). This enzymatic profile was used to contextualize the degradative capacity of each isolate and to generate preliminary hypotheses regarding the biochemical mechanisms underlying plastic-substrate utilization, particularly the relative contribution of esterolytic and lipolytic activity, which are most directly implicated in the hydrolysis of ester-containing and surface-oxidized polyolefin substrates.

2.3 Molecular identification of plastic-associated isolates

Genomic DNA extraction and quantification. Isolates demonstrating consistent growth on MSM-LDPE and favourable enzymatic profiles were selected for molecular identification, performed at Biokart India Pvt. Ltd. (Bengaluru, India). Genomic DNA was extracted from pure bacterial cultures using Xploregen gDNA extraction buffers following the manufacturer's standardized lysis-purification-elution workflow, and extracted DNA was quantified to confirm suitability for downstream polymerase chain reaction (PCR) amplification and sequencing. PCR amplification of the 16S rRNA gene was performed using a universal bacterial primer pair (forward: 5′-GGATGAGCCCGCGGCCTA-3′, Tm 57°C; reverse: 5′-CGGTGTGTACAAGGCCCGG-3′, Tm 58°C) under standard thermocycling conditions with an annealing temperature of 50°C. Amplicon size and integrity were verified by agarose gel electrophoresis prior to purification and sequencing.

Sequencing, alignment, and phylogenetic analysis. Confirmed PCR products were purified and sequenced on an ABI 3130xl Genetic Analyzer using Big Dye Terminator v3.1 chemistry. The resulting sequences were processed and aligned using SeqScape v5.2 software and compared against reference sequences in the National Center for Biotechnology Information (NCBI) nucleotide database using the Basic Local Alignment Search Tool (BLAST) to identify the closest bacterial homologues and establish taxonomic identity at the species or genus level. To further resolve the evolutionary placement of each isolate, phylogenetic relationships among the isolates and their closest reference sequences were inferred using the Neighbour-Joining method in MEGA 12 software, with bootstrap resampling performed to assess the statistical robustness of the inferred topology (Bruno et al. 2000). This combined approach of sequence-similarity searching and phylogenetic reconstruction allowed confident assignment of isolate identity while also situating each strain within its broader taxonomic and evolutionary context relative to previously reported plastic-associated bacteria.

2.4 Evaluation of LDPE transformation

Plastic pre-treatment. LDPE film was selected as the model substrate for biodegradation assays given its predominance in single-use plastic waste and its well-documented environmental persistence. Prior to use, LDPE pieces were thoroughly washed with distilled water to remove surface debris, treated with 70% ethanol to eliminate surface-associated contaminants, and subsequently UV-irradiated to achieve surface sterilization,

thereby ensuring that any growth or chemical change subsequently detected was attributable to the inoculated isolate rather than to indigenous surface flora present on the plastic at the outset.

LDPE treatment assay design. The transformation-associated response of the identified isolates was evaluated in MSM broth containing pre-treated, UV-sterilized LDPE films (2 × 2 cm) as the nominal sole external carbon source. Five LDPE pieces were introduced into each flask and cultures were incubated statically for 45 days. Uninoculated MSM-LDPE flasks were maintained in parallel as negative controls for abiotic changes in film mass and chemistry. Three independent biological replicates were performed for each isolate, with five LDPE films per replicate. Because gravimetric loss can arise from biological transformation, physical erosion or removal of additives, weight loss was interpreted together with FTIR and microscopy rather than as definitive evidence of complete mineralization.

Gravimetric analysis. LDPE pieces were weighed before inoculation and again after 45 days. Retrieved films were washed with distilled water and ethanol, UV-treated to remove adherent biomass, and dried at 25 ± 2 °C before weighing. Percentage weight loss was calculated as (Wi − Wf)/Wi × 100, where Wi is the initial mass and Wf is the final mass (Ali et al. 2021). The resulting values are referred to as apparent mass loss where appropriate, because gravimetry alone does not distinguish polymer assimilation from other sources of mass change.

$$Weight\ loss\ (\%)\ =\ \frac{W_i\ -\ W_f}{W_i}\ \times\ 100$$

where W_i represents the initial (pre-incubation) weight and W_f represents the final (post-incubation) weight of the LDPE sample (Ali et al. 2021).

Light microscopic examination of LDPE surface. Following retrieval and gentle washing as described above, a subset of bacteria-treated and untreated control LDPE fragments was additionally examined under a bright-field light microscope to assess surface-level changes associated with bacterial colonization. Films were visually inspected for evidence of bacterial attachment, biofilm formation, and physical surface alterations, including pitting, roughening, and fissuring, with untreated control films examined in parallel for comparison.

Scanning Electron Microscopy (SEM) analysis: selected bacterial cultures were grown on sterile polyethylene (PE) film squares (approx. 1x1 cm) placed on MSM agar plates for 7 days at 30°C. The colonized PE films were gently washed with sterile phosphate-buffered saline (PBS, pH 7.4), fixed overnight at 4°C in 2.5% glutaraldehyde in 0.1 M PBS, followed by post-fixation in 1% osmium tetroxide for 1 hour. Samples were then dehydrated through an ethanol series (30%, 50%, 70%, 90%, 100% for 15 min each), critical-point dried using a CO2 critical point dryer (Leica EM CPD300), and finally sputter-coated with a thin layer of gold-palladium using a high-vacuum sputter coater (Quorum Q150R ES). Micrographs were acquired using a scanning electron microscope (FEI Apreo S, operating at 5 kV).

FTIR spectroscopic analysis. Because gravimetric loss alone cannot establish polymer assimilation, FTIR was used to assess chemical changes in treated LDPE relative to uninoculated controls. Washed and dried films were analysed on a Bruker Alpha FTIR spectrometer over 4000--500 cm^{-1}. Changes in characteristic carbonyl and hydroxyl regions were evaluated, and Carbonyl Index (CI) and Hydroxyl Index (HI) were calculated relative to the methylene reference band near 1463 cm^{-1}. Increased CI or HI was interpreted as evidence of oxidation or introduction of oxygen-containing functional groups into the polymer surface. These data provide chemical support for polymer modification but do not, by themselves, identify the enzymes responsible or demonstrate complete mineralization.

2.5 Statistical analysis

All experiments were performed in triplicate (three independent biological replicates). Results are expressed as mean values± standard error. Data were analysed using SPSS and Microsoft Excel, with differences among treatments evaluated by one-way analysis of variance (ANOVA) followed by Tukey's multiple comparison test, statistical significance being set at $p < 0.05$. F-statistics, degrees of freedom, and exact p-values for each

comparison are reported alongside the corresponding results. Graphical representations of growth curves, dose-response relationships, and enzymatic profiles were generated using Microsoft Excel.

3. Results

3.1 Isolation and mass culturing of bacterial isolates

Serial dilution and spread-plating of soil samples collected from the plastic-contaminated dumping site yielded a heterogeneous bacterial population on Luria-Bertani (LB) agar, with colonies differing significantly in pigmentation, size, texture, elevation, and margin morphology. From this population, four morphologically distinct isolates were selected for further characterization on the basis of consistent and reproducible colony phenotypes: a white colony (designated DW), a pink colony (DP), a yellow colony (DY), and a light-yellow colony (DLY) (Fig. 1). Each isolate was purified by repeated streak-plating until axenic cultures with uniform colony characteristics were obtained, and subsequently mass-cultured in Luria-Bertani (LB) broth to generate sufficient biomass for downstream biochemical, molecular, and biodegradation assays. All four isolates exhibited visible turbidity and dense growth in LB broth within the incubation period, confirming successful establishment of pure cultures suitable for further study.

Fig. 1. Morphologically distinct bacterial isolates exhibiting white (DW), pink (DP), yellow (DY), and light-yellow (DLY) colony pigmentation, isolated from landfill soil samples and purified on Luria–Bertani (LB) agar medium.

3.2 Microscopic characterization

Gram staining of the four purified isolates revealed a consistent cellular phenotype across all strains. Each isolate stained pink under oil-immersion microscopy (100× objective; total magnification, 1000×), indicating a Gram-negative cell-wall composition, and each displayed a rod-shaped cellular morphology (Fig. 2). The uniformity of Gram reaction and cell shape across otherwise pigment-distinct isolates suggested that, despite their colony-level phenotypic diversity, the four studied strains share a broadly similar structural cell-envelope architecture a finding consistent with their subsequent molecular identification as members of Gram-negative genera. This microscopic confirmation of purity and morphological consistency provided the necessary basis for proceeding to physiological optimization and downstream characterization.

Fig. 2. Gram staining of the four purified bacterial isolates showing Gram-negative, rod-shaped morphology under oil-immersion microscopy. Microscopy was performed using a 100× oil-immersion objective (total magnification 1000×).

3.3 Optimization of physical growth parameters

Effect of temperature. Growth of the four isolates was evaluated across a temperature gradient of 20--35°C, with bacterial density quantified spectrophotometrically (OD_{610}). All isolates displayed a consistent mesophilic growth pattern, with maximum biomass accumulation recorded at 30°C and a marked decline in growth at both lower (20°C, 25°C) and higher (35°C) temperatures (Fig. 3). Among the four strains, the light-yellow isolate (DLY) exhibited the highest absorbance at the optimum temperature (OD_{610} = 1.146± 0.05), followed by the yellow isolate DY (0.934 ± 0.03), the white isolate DW (0.863 ±0.02), and the pink isolate DP (0.830 ± 0.03) (Fig. 3). This convergence on a shared temperature optimum of 30°C indicates that the isolated strains are well adapted to ambient soil and environmental temperatures typical of the sampling site, and supports their potential suitability for future biotransformation applications under moderate, field-relevant thermal conditions rather than requiring specialized incubation regimes.

Fig. 3. Growth pattern of bacterial isolates measured as absorbance at 610 nm (OD_{610}) under different physiological conditions. (A) Effect of temperature (20, 25, 30, and 35°C). (B) Effect of pH (5, 6, 7, and 8). Bars

represent mean growth values ± SE. Different lowercase letters indicate statistically significant differences among treatments according to one-way ANOVA followed by Tukey's HSD post hoc test ($P < 0.05$).

Effect of pH. The growth response of the four bacterial isolates was evaluated across a pH gradient of 5--8, revealing a common optimum at pH 7.0 (Fig. 3). At the optimum pH, the recorded absorbance (OD_{610}) values were 0.734± 0.01 for DW, 0.438± 0.011 for DP, 0.440± 0.01 for DY, and 0.706 ± 0.02 for DLY. Growth was markedly reduced under both acidic (pH 5-6) and alkaline (pH 8) conditions, indicating that deviation from neutrality adversely affected bacterial proliferation. The white (DW) and light-yellow (DLY) isolates exhibited the highest growth at pH 7.0, 0.734± 0.012, 0.706 ± 0.011 respectively consistent with the trend observed during temperature optimization. These findings demonstrate that 30°C and pH 7.0 constitute the optimum physiological conditions for the growth of all four isolates. Accordingly, these conditions were selected for all subsequent biodegradation experiments to ensure that LDPE transformation reflected the intrinsic metabolic and enzymatic capabilities of the isolates rather than physiological stress.

To further characterize the growth behaviour of the isolates under their optimized culture conditions, all four strains were cultivated in Luria-Bertani (LB) broth at 30°C and pH 7.0, and their growth kinetics were monitored over time (Fig. 4). Bacterial growth was quantified by measuring the optical density at 610 nm (OD_{610}) at regular intervals. The growth curves shown in Fig 4 represent the mean values of three independent biological replicates, thereby ensuring the reproducibility and reliability of the observed growth patterns.

Fig. 4. Growth kinetics of bacterial strains measured as absorbance at 610 nm (OD_{610}) over six days. Values represent mean ± SE ($n = 3$). Distinct symbols/lines represent Pink (DP), White (DW), Yellow (DY), and Light-yellow (DLY) isolates. Statistical differences were evaluated by one-way ANOVA followed by Tukey's multiple comparison test ($P < 0.05$); significance annotations are retained only where relevant for visual clarity.

3.4 Comparative growth in nutrient-rich and nutrient-deficient media

To evaluate the capacity of the isolates to tolerate nutrient restriction a condition directly relevant to their potential use of plastic as a carbon source growth was compared between nutrient-rich LB medium and nutrient-deficient Minimal Salt Medium (MSM), both in the presence and absence of supplemented LDPE. As expected, all four isolates exhibited substantially higher growth in LB medium than in plain MSM, with the light-yellow isolate again showing the greatest biomass accumulation in LB ($OD_{610} = 0.847$) (Fig. 5). Growth in unsupplemented MSM was markedly reduced across all isolates, consistent with the absence of a readily metabolizable carbon source in this minimal formulation. When LDPE plastic was introduced into MSM as the sole carbon source, all four isolates displayed a gradual but consistent increase in absorbance over the six-day monitoring period, indicating sustained viability and growth in a medium where plastic represented the only available carbon input (Fig. 6). Among the isolates, the white (DW) and light-yellow (DLY) strains showed comparatively greater growth in MSM-LDPE relative to the pink and yellow isolates, suggesting a correspondingly higher capacity to utilize the plastic substrate. This progressive, if reduced, growth in MSM-LDPE is consistent with plastic-associated growth potential, although residual inoculum-derived nutrients cannot be fully excluded, and it informed isolate selection for the downstream molecular and degradation analyses described below.

Fig. 5. Comparative growth of bacterial isolates in Luria–Bertani (LB) medium and Minimal Salt Medium (MSM), measured as absorbance at 610 nm (OD_{610}). The figure compares growth under nutrient-rich LB and nutrient-limited MSM conditions.

Fig. 6. Growth of bacterial isolates on Minimal Salt Medium (MSM) supplemented with plastic. **(A)** Growth on MSM agar plates showing colony development of Light-yellow (DLY), White (DW), Yellow (DY), and Pink (DP) isolates in the presence of plastic. **(B)** Growth of the different bacterial strains in MSM liquid media containing plastic substrate, showing visible turbidity differences among the four isolates relative to the uninoculated control.

3.5 Molecular identification of bacterial isolates

Genomic DNA extracted from the four purified isolates yielded a working concentration of 164 ng/µL, confirmed as suitable for PCR amplification and sequencing. Amplification of the 16S rRNA gene using the primer pair and cycling conditions described in Section 2.3 produced amplicons of the expected size for all four isolates, as confirmed by agarose gel electrophoresis. Sequencing on the ABI 3130xl platform, followed by BLAST analysis against the NCBI nucleotide database, identified the four isolates as follows (Table 1): the white isolate (DW) was most closely related to *Pseudomonas* sp.; the pink isolate (DP) showed closest similarity to *Dyella japonica*; the light-yellow isolate (DLY) was identified as *Enterobacter* sp. (closest match, *Enterobacter* sp. strain S1 DTA); and the yellow isolate (DY) was identified as *Pantoea agglomerans* (Fig. 7).

Table 1. Summary of the closest BLASTn matches of the 16S rRNA gene sequences of DDUC bacterial isolates, showing the nearest taxonomic affiliations, percentage sequence identity, and confidence level of species identification based on sequence similarity.

Isolate	Closest BLAST match(es)	% Identity Range*	Confidence
White Strain (DW)	*Pseudomonas* sp.	99.2–99.8%	High
Pink Strain (DP)	*Dyella japonica*	99.1–99.8%	High
Light Yellow (DLY)	*Enterobacter hormaechei*	99.0–99.7%	High
Yellow Strain (DY)	*Pantoea agglomerans*	98.5–99.3%	High

**Confidence levels were assigned based on sequence similarity and phylogenetic clustering, where ≥99% identity indicates high confidence in species-level assignment.*

Fig. 7. Phylogenetic trees constructed using 16S rRNA gene sequences showing the evolutionary relationships of DDUC bacterial isolates with their closest relatives retrieved from the NCBI GenBank database. Bootstrap values (shown at the nodes) were obtained from 1,000 replicates. **Bootstrap value interpretation: ≥90%** = High support; **70–89%** = Moderate support; **<70%** = Low support.

Phylogenetic reconstruction using MUSCLE multiple sequence alignment and the Neighbor-Joining method placed all four isolates within well-supported clades alongside their closest NCBI reference homologues, with bootstrap analysis lending statistical confidence to the inferred topology (Fig. 7). The clustering of each isolate with its corresponding reference taxon corroborated the BLAST-based identification and confirmed the taxonomic assignment of all four strains. All four identified genera *Pseudomonas*, *Dyella*, *Enterobacter* and *Pantoea* are widely recognized as environmentally versatile, metabolically adaptable taxa with documented roles in xenobiotic degradation and bioremediation, lending biological plausibility to the plastic-associated growth phenotypes observed in the preceding growth assays.

3.6 Biosafety-associated phenotypic screening

Given the intended downstream application of these isolates in environmental bioremediation, their pathogenic potential was assessed through a standard panel of biochemical assays (Table 2). All four isolates returned a negative Indole test result, indicating limited or absent tryptophanase activity. Methyl Red (MR) testing yielded positive results for DW, DY, and DP, consistent with stable mixed-acid fermentation end products, whereas DLY returned a negative MR result, pointing to divergent carbohydrate fermentation pathways among the isolates. All four strains were negative for the Voges-Proskauer test, indicating that none of the isolates utilize the butylene-glycol fermentation pathway under the conditions tested. Conversely, all isolates tested positive for citrate utilization, evidenced by a green-to-blue colour transition on Simmons' citrate agar, demonstrating an ability to use citrate as a sole carbon source and indicating broad metabolic versatility consistent with their subsequent plastic-associated growth phenotype.

Table 2. Environmental Characterization of Four Bacterial Isolates Based on Growth Under Different Physicochemical Conditions

Biochemical Test	DW (*Pseudomonas aeruginosa*)	DP (*Dyella japonica*)	DLY (*Enterobacter* sp. strain S1 DTA)	DY (*Pantoea agglomerans*)
Indole Test	-	-	-	-
Methyl Red Test	+	+	-	+
Voges Proskauer Test	-	-	-	-
Citrate Test	+	+	+	+
Blood Agar Test	-	-	-	-
DNase Agar Test	-	-	-	-

(-) = Negative response, (+) = Positive response

All four isolates were negative for haemolysis and DNase under the conditions tested. These findings indicate that the selected isolates did not express the two phenotypic markers examined in this screening panel. They should not, however, be interpreted as proof of non-pathogenicity or unrestricted environmental safety; such conclusions require broader genomic, physiological and risk-assessment approaches. This distinction is particularly important for isolates assigned to taxa with recognized opportunistic pathogenic members.

3.7 Antibiotic sensitivity profile

Disc-diffusion assays on Mueller–Hinton agar revealed clear isolate-specific variation in antibiotic susceptibility (Fig. 8). The white isolate (DW) showed its highest susceptibility to cefepime and penicillin, with inhibition zones of 20 mm and 18 mm, respectively. The light-yellow isolate (DLY) displayed the largest overall zone of inhibition (22 mm, chloramphenicol), indicating the highest relative antibiotic susceptibility among the four strains. The pink isolate (DP) behaved as a multidrug-resistant strain, with inhibition zones of only 0–5 mm, whereas the yellow isolate (DY) showed moderate sensitivity to neomycin (14 mm) and streptomycin (13 mm). This differential susceptibility pattern across isolates reflects natural variation in antibiotic resistance mechanisms among environmentally derived strains and provides a useful baseline antimicrobial profile, supporting the overall characterization of these isolates as a precondition for their safe handling and application.

Fig. 8. Antibiotic sensitivity test on Mueller-Hinton agar showed highest susceptibility in White (DW) strain to Cefepime (20 mm) and Penicillin (18 mm), Light Yellow (DLY) Strain to Chloramphenicol (22 mm), Pink (DP) strain as multidrug-resistant (0–5 mm zones), and Yellow strain (DY) with moderate sensitivity to Neomycin (14 mm) and Streptomycin (13 mm).

3.8 Biochemical and enzymatic characterization

Enzymatic profiling under LB and MSM conditions revealed clear isolate- and medium-dependent differences (Table 3). Catalase activity was detected in all isolates under both conditions. Cellulase activity was detected in DW and DLY, α-amylase activity in DW and DY, and protease activity in DW and DY. The most notable difference concerned lipase/esterase activity: it was detected only in DW and only after growth under MSM conditions. No lipase/esterase activity was detected for DP, DY or DLY under either medium. This pattern is consistent with condition-dependent expression of an esterolytic phenotype in DW. It provides a testable biochemical association with the stronger oxidative signature observed later by FTIR, but the plate assay does not establish that the detected activity acts directly on LDPE or that it represents the complete degradation mechanism.

Table 3. Comparative Analysis of Biochemical Traits and Extracellular Enzyme Activities of Bacterial Isolates Cultivated in LB and MSM Media

Biochemical test	Grown in LB medium				Grown in MSM medium			
	DW	DP	DY	DLY	DW	DP	DY	DLY
Catalase Test	++	++	++	++	+	+	+	+
Cellulase Test	++	-	-	++	+	-	-	++
Alpha Amylase Test	++	-	++	-	+	-	+	-
Protease Test	++	-	++	-	++	-	++	-
Lipase/Esterase Test	-	-	-	-	++	-	-	-

3.9 LDPE transformation assessment

After 45 days under the selected conditions (30 °C, pH 7, MSM), the pooled LDPE mass decreased from 44.2 ± 1.5 mg to 38.2 ± 1.1 mg, corresponding to a net reduction of 6.0 mg and an overall apparent mass loss of 13.6% (Fig. 9). No detectable mass change was reported for the uninoculated control. The absence of mass change in the uninoculated control, in contrast to the loss in the inoculated flasks, supports a biological contribution to the observed mass change, while the FTIR and microscopy results below provide additional evidence of polymer surface modification.

Fig. 9. Initial weight, final weight, and apparent percentage mass loss of the LDPE substrate following treatment with bacterial isolates Pink (DP), White (DW), Yellow (DY), and Light Yellow (DLY). Values are presented as mean ± SE. Different lowercase letters above bars indicate significant differences among bacterial strains according to one-way ANOVA followed by Tukey's HSD test at $P < 0.05$.

Comparative analysis of the four isolates revealed clear differences in apparent LDPE mass loss. A one-way analysis of variance (ANOVA) revealed that bacterial strain had a highly significant effect on apparent LDPE mass loss, as measured by apparent percentage mass loss ($F_{3,8} = 128.18$, $P < 0.001$). Among the four isolates, DW exhibited the highest apparent mass loss (16.07 ± 0.18%), followed by DLY (13.96 ± 0.14%), DY (12.39 ± 0.24%), and DP (11.82 ± 0.09%). Subsequent multiple comparison analysis (Tukey's honestly significant difference test, $P < 0.05$) confirmed that all four strains differed significantly from one another, indicating distinct apparent mass-loss responses among the isolates.

3.10 FTIR spectroscopic analysis of LDPE films

FTIR spectroscopy was performed to characterize chemical changes in the LDPE polymer backbone induced by bacterial treatment, with spectra of bacteria-treated films compared against untreated control films across the 4000--500 cm^{-1} range (Fig. 10). The control LDPE film displayed a spectral profile typical of unmodified polyethylene, with characteristic absorption bands corresponding to O-H stretching (3200--3600 cm^{-1}), asymmetric and symmetric C--H stretching (2915-2920 cm^{-1} and 2845--2850 cm^{-1}, respectively), carbonyl (C=O) stretching (1710--1745 cm^{-1}), C-H bending (1460--1470 cm^{-1}), and C-H rocking (718-725 cm^{-1}) vibrations.

Fig. 10. FTIR spectra of untreated control and bacterial-treated LDPE films [Pink (DP), Light-yellow (DLY), Yellow (DY), and White (DW)] showing isolate-associated changes in absorption bands related to oxygen-containing functional groups. The corresponding Carbonyl Index (CI) and Hydroxyl Index (HI) values are: control, CI = 0.1199 and HI = 0.0594; DP, CI = 0.1602 and HI = 0.0992; DLY, CI = 0.2031 and HI = 0.0637; DY, CI = 0.1511 and HI = 0.0337; and DW, CI = 0.2444 and HI = 0.1773. The x-axis represents wavenumber (cm^{-1}).

Following bacterial treatment, isolate-specific shifts in peak position, intensity, and transmittance were observed relative to the control spectrum, particularly within the carbonyl and hydroxyl absorption regions, indicating oxidative modification of the polymer surface. To quantify these changes, Carbonyl Index (CI) and Hydroxyl

Index (HI) values were calculated for the control and each bacterially treated sample (Table 4). The control film exhibited baseline CI and HI values of 0.1199 and 0.0594, respectively, reflecting the absence of pre-existing oxidation.

Table 4. FTIR-based assessment of carbonyl index (CI), hydroxyl index (HI), and structural modifications in LDPE films following bacterial treatment.

Sample	CI	HI	Inference
Control (c)	0.1199	0.0594	Baseline plastic; no oxidation.
White (DW)	**0.2444**	**0.1773**	Highest oxidation; most effective.
Light Yellow (DLY)	0.2031	0.0637	Moderate oxidation & chain scission.
Pink (DP)	0.1602	0.0992	Early surface modification.
Yellow (DY)	0.1511	0.0337	Minimal interaction; mostly stable.

DW produced the largest FTIR response, with CI = 0.2444 and HI = 0.1773 compared with 0.1199 and 0.0594 in the control. DLY also showed a marked increase in CI (0.2031), but only a small increase in HI (0.0637). DP had intermediate CI and HI values (0.1602 and 0.0992), whereas DY showed the smallest departure from the control (CI = 0.1511; HI = 0.0337). The ranking of CI broadly followed the gravimetric response, with DW highest and DLY second. Importantly, the FTIR results demonstrate isolate-dependent chemical modification of the LDPE surface; they do not by themselves establish the identity of the oxidizing enzymes or the sequence of reactions leading from surface oxidation to carbon assimilation.

The FTIR data provide complementary evidence of chemical modification of the LDPE surface alongside the gravimetric and microscopic observations. The white isolate (DW), in particular, exhibited both the highest gravimetric weight loss and the highest Carbonyl and Hydroxyl Indices, indicating that enhanced oxidative modification of the polymer surface was accompanied by greater overall degradation. These findings are consistent with the exclusive induction of lipase/esterase activity in DW under MSM conditions and are consistent with an association between the measured extracellular enzyme phenotype and oxidative polymer modification; the present data do not establish a causal mechanism.

3.11 Scanning electron microscopy (SEM) analysis of bacterial colonization

SEM revealed isolate-dependent differences in surface colonization (Fig. 11). All four isolates formed cell aggregates associated with an extracellular polymeric substance (EPS)-rich matrix on the PE surface, but the density and continuity of coverage varied. DW showed the most extensive and multilayered appearance, whereas DP and DY showed thinner, more discontinuous colonization; DLY displayed an intermediate pattern. The SEM observations therefore support a relationship between the extent of surface-associated biofilm and the magnitude of degradation-related responses. Because SEM provides a structural rather than functional measurement, these images are interpreted as evidence of colonization and biofilm formation, not as direct proof that EPS itself caused polymer chain cleavage.

Fig. 11. Scanning electron micrographs (SEM) of bacterial isolates colonizing separate polyethylene (PE) film squares used for SEM analysis. Panels: (A) White isolate (DW), 1.50 kX; (B) Pink isolate (DP), 1.50 kX; (C) Light-yellow isolate (DLY), 10.00 kX; and (D) Yellow isolate (DY), 20.00 kX. Scale bars: 1 µm. The SEM substrate was PE film used specifically for the 7-day SEM colonization assay and was not the 45-day LDPE film used for the gravimetric LDPE gravimetric assay.

3.12 Light microscopic examination of LDPE film surfaces

Bright-field microscopy of the LDPE films after 45 days of incubation provided supporting visual evidence of surface-associated transformation (Fig. 12). Films incubated with the four isolates showed representative surface

irregularities and roughening, and films incubated with the light-yellow isolate displayed clear evidence of bacterial attachment and surface colonization, in contrast to the untreated control films, which retained a smooth, unaltered surface free of microbial colonization. This surface-level evidence of bacterial adhesion and physical alteration of the plastic substrate is consistent with the biofilm-mediated mechanism of attachment, colonization, and progressive surface erosion characteristic of microbial plastic transformation, and reinforces the gravimetric findings. Because light microscopy resolves only gross topographical change, these observations were interpreted together with the SEM and FTIR results described above.

Fig. 12. Representative bright-field microscopic observations of LDPE films after 45 days of incubation. Panels: (A) White colony (DW), (B) Pink colony (DP), (C) Yellow colony (DY), and (D) Light-yellow colony (DLY), illustrating representative surface morphological alterations, including roughening and irregularities where visible. The LDPE transformation experiment comprised three independent biological replicates; the images shown are representative fields.

4. Discussion

The central finding of this study is not the discovery of another LDPE-associated isolate, but the functional variation observed when four isolates from the same plastic-contaminated landfill were evaluated side-by-side. The isolates shared broad physiological features---most notably an optimum around 30 °C and pH 7---but differed in LDPE-associated mass loss, extracellular enzyme profiles, surface colonization and FTIR oxidation indices. This combination is informative because studies of polyethylene biodegradation often emphasize the best-performing isolate, whereas a comparative design can reveal whether apparently similar degraders have similar phenotypes. Recent landfill and mixed-culture studies have already demonstrated that LDPE transformation can be associated with biofilm formation, FTIR-detectable oxidation and, in some systems, substantially enhanced performance of mixed communities (Merchant et al. 2025; Ting and Sallahudin 2025; Tirkey and Upadhyay 2025; Uddin et al. 2025; Zhang et al. 2025; Abisha et al. 2026). The present work complements that literature by focusing on isolate-level heterogeneity within a single source habitat and by asking how measurable phenotypic traits covary across the isolates.

4.1 Isolation, morphological diversity, and environmental adaptation

Four colony morphotypes were recovered from the same plastic-contaminated landfill and purified for comparative analysis. The recovery of *Pseudomonas*, *Dyella*, *Enterobacter* and *Pantoea* affiliated isolates is consistent with the broad taxonomic diversity reported from plastic-rich waste environments. Importantly, the taxonomic identities themselves are not treated as the principal novelty because *Pseudomonas* and *Enterobacter* have already been studied in Indian LDPE systems (Sarker et al. 2020; Shilpa et al. 2024; Sharma and Neelam 2025). Rather, their co-occurrence at one landfill provides a controlled ecological context in which differences in measurable transformation-associated phenotypes can be compared without changing the sampling environment. This design allowed us to ask whether isolates sharing the same contaminated habitat nevertheless differ in the functional traits associated with LDPE transformation.

All four isolates were Gram-negative rods. Although Gram-negative bacteria, including *Pseudomonas* and *Enterobacter*, are frequently represented in studies of plastic-associated microbial communities, cell morphology alone provides little mechanistic information about polymer transformation. In the present study, the value of the morphological observation is therefore mainly as a baseline descriptor that, when combined with the later molecular, enzymatic, SEM and FTIR data, helps define the phenotype of each isolate.

4.2 Growth optimization and carbon-source utilization

All four isolates grew best at 30 °C and pH 7, indicating broadly similar physiological optima despite their later differences in transformation-associated traits. The convergence is useful experimentally because subsequent LDPE assays were performed under a common set of conditions, reducing the possibility that differences in mass loss simply reflected different growth optima. At the same time, the highest biomass producer was not necessarily

the highest apparent mass-loss response, showing that general growth capacity and polymer-associated performance should not be treated as interchangeable traits.

Growth in MSM supplemented with LDPE was sustained over the observation period, particularly for DW and DLY. This result supports the ability of these isolates to remain metabolically active under nutrient-limited, plastic-containing conditions. However, growth in such a system is not equivalent to demonstrated assimilation of polymer carbon because residual nutrients from the inoculum or utilization of low-molecular-weight compounds released from the plastic can contribute to biomass formation. The stronger evidence comes from the convergence of growth with gravimetric loss, surface colonization and FTIR-detected chemical modification. This distinction is important for interpreting the present results conservatively.

4.3 Molecular taxonomy and associated physiological traits

16S rRNA sequencing assigned the isolates to *Pseudomonas* sp. (DW), *Dyella japonica* (DP), *Enterobacter* sp. (DLY) and *Pantoea agglomerans* (DY). The four genera are represented to very different extents in the plastic-biodegradation literature. LDPE transformation by *Pseudomonas aeruginosa* WD4, isolated from a plastic dumpsite, and by *Enterobacter cloacae* AKS7 has been documented in India (Sarker et al. 2020; Shilpa et al. 2024), and *Enterobacter* sp. has also been reported among LDPE-transforming isolates from a waste-disposal site (Sharma and Neelam 2025). *Pantoea* strains have been reported to degrade LDPE (Skariyachan et al. 2016; de Fretes et al. 2024), whereas *Dyella* sp. has so far been detected only within mixed bacterial assemblages degrading polyethylene and other microplastics (Ren and Ni 2023). Accordingly, *Pseudomonas* and *Enterobacter* are not presented here as taxonomic novelties, and the same applies to *Pantoea* at genus level. Our targeted literature search did not identify an earlier LDPE study of a *Dyella japonica* or *Pantoea agglomerans* isolate; to our knowledge, DP and DY therefore provide the first species-level LDPE-associated phenotypes for these two taxa, although the absence of an identified report cannot be taken as proof that none exists. Their inclusion alongside DW and DLY in a single within-site comparison, with contrasting combinations of apparent mass loss, FTIR oxidation indices, EPS-rich biofilm architecture and extracellular-enzyme phenotypes, constitutes the principal contribution of this work.

4.4 Biochemical profile, environmental safety, and enzymatic capacity

The biochemical assays demonstrated broad metabolic diversity among the isolates, but the most informative observation for the study hypothesis was the selective appearance of lipase/esterase activity in DW under MSM conditions. This association is consistent with the idea that nutrient limitation or plastic exposure can alter extracellular enzyme expression. It should not, however, be interpreted as evidence that a particular lipase or esterase is an LDPE depolymerase. LDPE is a polyolefin lacking the ester bonds characteristic of polyester substrates, and oxidation of the polyethylene surface may generate chemically different targets for subsequent attack. Thus, the present assay is best regarded as a functional marker associated with the DW phenotype, and the observed relationship should be tested with quantitative enzyme assays, secretome analysis or gene-level approaches in future work.

The antibiotic susceptibility profiles provide additional phenotypic information but are not central to the LDPE transformation mechanism. More importantly, the haemolysis and DNase results should be interpreted only as limited biosafety screening. They support the absence of the two phenotypes tested, but they do not establish that the isolates are non-pathogenic or suitable for unrestricted environmental release. This qualification applies across all four isolates, and species-level identification of each isolate should be taken into account when assessing biosafety before any environmental application is considered.

4.5 Gravimetric analysis and surface colonization of LDPE films

After 45 days, all four isolates produced measurable LDPE mass loss relative to the uninoculated control, with DW showing the highest value (16.07%), followed by DLY (13.96%), DY (12.39%) and DP (11.82%). The magnitude of the differences is important because the isolates were evaluated under the same temperature, pH,

medium and incubation period. The data therefore support strain-specific differences in performance rather than simply differences caused by experimental conditions. Nevertheless, the absolute values should be interpreted in the context of the 45-day laboratory assay and should not be extrapolated directly to field-scale degradation rates. Recent studies have reported both lower and substantially higher LDPE losses depending on the organism, enrichment strategy, incubation period and analytical depth (Merchant et al. 2025; Ting and Sallahudin 2025; Tirkey and Upadhyay 2025; Uddin et al. 2025; Zhang et al. 2025; Abisha et al. 2026), reinforcing the need to compare degradation percentages only when experimental designs are closely matched.

DW was the strongest performer, whereas DLY was a close second despite lacking detectable lipase/esterase activity. This contrast is more informative than the absolute ranking itself. It suggests that a single plate-based enzyme marker cannot account for all of the observed variation in LDPE-associated mass loss. DLY may rely on other extracellular activities, oxidative processes, surface-active metabolites, or physical effects associated with biofilm formation. The current dataset cannot distinguish among these possibilities, but it establishes a clear experimental question for follow-up work.

Light microscopy showed bacterial attachment and visible surface irregularities on treated films, whereas the untreated control remained comparatively smooth. These observations are consistent with surface colonization, but microscopic roughening alone cannot distinguish biological erosion from other physical changes. Their evidentiary value therefore comes from their agreement with the gravimetric and FTIR measurements rather than from the images considered in isolation.

4.6 Scanning electron microscopic evidence of biofilm ultrastructure

SEM added structural evidence for the isolate-specific nature of surface colonization. The presence of bacterial cells within an EPS-rich matrix is consistent with biofilm formation at the polymer interface. DW displayed the most extensive coverage, which is concordant with its higher mass loss and stronger FTIR response. DLY showed an intermediate colonization phenotype despite being esterase-negative. These observations support a model in which biofilm formation is an important enabling trait, while the chemical route from surface colonization to polymer transformation may differ among isolates.

The strength of the present result lies in the convergence of independently measured phenotypes: gravimetric response, enzyme induction, FTIR oxidation and SEM-based colonization. Similar combinations of techniques have been used in recent LDPE studies, including landfill-derived isolates and mixed cultures (Merchant et al. 2025; Ting and Sallahudin 2025; Tirkey and Upadhyay 2025; Uddin et al. 2025; Zhang et al. 2025; Abisha et al. 2026). What the present comparison adds is the explicit within-site contrast. DW combines extensive biofilm formation, detectable MSM-induced lipase/esterase activity and the strongest oxidative and gravimetric responses, whereas DLY combines substantial mass loss and carbonyl formation with no detectable lipase/esterase activity. The appropriate interpretation is therefore not that two complete transformation pathways have been resolved, but that the isolates exhibit distinct, experimentally measurable phenotypic signatures associated with LDPE transformation.

4.7 FTIR spectroscopic evidence of polymer oxidation

FTIR showed isolate-dependent increases in oxygen-containing functional groups, with DW producing the highest CI and HI and DLY showing a relatively high CI but only a modest HI increase. These patterns are consistent with oxidative modification of the polyethylene surface and agree with the gravimetric ranking. The results are also in line with recent work in which FTIR has been used alongside SEM and mass-loss measurements to support LDPE transformation (Merchant et al. 2025; Ting and Sallahudin 2025; Tirkey and Upadhyay 2025; Uddin et al. 2025; Zhang et al. 2025; Abisha et al. 2026). Importantly, FTIR should be viewed as evidence of chemical modification rather than a direct map of the biotransformation pathway. The formation of carbonyl and hydroxyl groups can result from oxidation at the polymer surface, but the present experiments do not establish whether the initiating reaction is enzymatic, radical-mediated, or associated with other extracellular processes.

The comparison between DW and DLY provides the clearest functional contrast in the dataset. DW combined the highest apparent mass loss (16.07%), the highest CI (0.2444), the highest HI (0.1773), the most extensive SEM-visible biofilm and the only detectable lipase/esterase activity under MSM conditions. DLY, in contrast, produced 13.96% mass loss and a CI of 0.2031 without detectable lipase/esterase activity, while showing intermediate surface colonization. We interpret this as evidence for two different measurable phenotypic profiles rather than two fully resolved biochemical pathways. A useful working model is that DW has a phenotype strongly associated with esterolytic activity and oxidative surface modification, whereas DLY achieves a similar endpoint through an as-yet-unresolved non-esterolytic route. This distinction is potentially relevant to consortium development, but synergy or improved performance of a DW--DLY consortium remains a hypothesis that must be tested experimentally.

4.8 Integrated interpretation

The combined dataset supports a useful distinction between apparent mass-loss magnitude and transformation-associated phenotype. DW was consistently strong across the measured indicators, whereas DLY reached a comparable level of apparent mass loss without detectable lipase/esterase activity. DP and DY showed comparatively lower responses across several measured endpoints. This pattern suggests that LDPE-associated performance is multidimensional: growth under nutrient limitation, surface colonization, extracellular enzyme expression and chemical oxidation need not vary in parallel. The study therefore provides a comparative phenotype map rather than a complete mechanistic pathway.

5. Conclusions

This study shows that indigenous bacteria recovered from the same plastic-contaminated landfill can differ markedly in the combination of traits associated with LDPE transformation. Under a common experimental condition, *Pseudomonas* sp. DW showed the highest apparent mass loss (16.07%), the strongest carbonyl and hydroxyl responses, the most extensive EPS-rich surface colonization and the only detectable lipase/esterase activity under MSM conditions. *Enterobacter* sp. DLY was particularly informative because it produced substantial mass loss (13.96%) and carbonyl formation despite no detectable lipase/esterase activity. Because *Pseudomonas* and *Enterobacter* associated LDPE transformation has already been documented in India (Sarker et al. 2020; Shilpa et al. 2024; Sharma and Neelam 2025), the principal contribution of this study is not the discovery of a new plastic-degrading genus or species. Instead, it is the comparative demonstration of within-site functional heterogeneity across four co-occurring isolates, including *Dyella japonica* and *Pantoea agglomerans*, which, to our knowledge, have not previously been characterised for LDPE transformation at species level, and the integrated phenotype map linking gravimetric response, extracellular-enzyme phenotype, biofilm architecture and FTIR-derived oxidation indices. The results further indicate that similar LDPE-associated endpoint responses can arise from different combinations of measurable microbial traits. The contrast between DW and DLY generates a testable hypothesis for future consortium studies: strains with complementary rather than redundant phenotypes may provide different functions during polymer transformation. This hypothesis was not tested in the present work. Future studies should therefore quantify extracellular enzyme activities, characterize secreted metabolites and degradation products, assess changes in molecular weight and crystallinity, and use genomic or metagenomic approaches to identify candidate oxidative and hydrolytic pathways. Direct comparison of individual strains with defined two- and multi-member consortia will be needed to determine whether the functional contrasts observed here translate into synergistic LDPE transformation.

Statements and Declarations

Funding. This research was supported by Deen Dayal Upadhyaya College, University of Delhi, which provided financial assistance for selected outsourced experimental analyses and laboratory-related expenses. No external funding was received.

Competing interests. The authors declare that they have no known competing financial interests or personal relationships that could have appeared to influence the work reported in this paper.

Ethics approval. Not applicable. This study did not involve human participants, human tissues, personal data, or experimental animals. The research involved environmental bacterial isolates obtained from municipal landfill soil samples.

Author contributions. Sandeep Kumar designed and supervised the study and carried out final editing of the manuscript. Alisha Srivastwa carried out all experiments and prepared the first draft. Sweta Singh collected soil samples, performed initial isolate purification and carried out electron microscopy. Harshita Singh assisted with literature review, data compilation and analysis. Syed Ali Abbas performed the antibiotic-sensitivity assay under the supervision of Ravinder Singh. All authors read and approved the final manuscript.

Data availability. The datasets generated and/or analysed during the current study are available from the corresponding author on reasonable request. The 16S rRNA gene sequences generated in this study have been deposited in GenBank under accession numbers [Pantoea agglomerans strain YCKS02 ACCESSION PV810110; Enterobacter sp. strain LYCKS04 ACCESSION PV810113]

References

Abisha RJ, Rani V, Manimekalai D, Muruganantham M (2026) Indigenous LDPE transformation bacteria from plastic dumping soils of Thoothukudi coast: isolation, characterization and degradation efficiency. *Arch Microbiol* 208(2):108. https://doi.org/10.1007/s00203-025-04666-9

Al-Ajeeli ZA (2024) Isolation and identification of some pathogenic and contaminated bacterial species for burns in the city of Hilla. *Int J Sci Acad Res* 5(1):6864–6869

Ali SS, Elsamahy T, Al-Tohamy R, Zhu D, Mahmoud YAG, Koutra E, Sun J (2021) Plastic wastes biodegradation: mechanisms, challenges and future prospects. *Sci Total Environ* 780:146590. https://doi.org/10.1016/j.scitotenv.2021.146590

Alshehrei F (2017) Biodegradation of synthetic and natural plastic by microorganisms. *J Appl Environ Microbiol* 5(1):8–19

Bakht A, Rasool N, Iftikhar S (2020) Characterization of plastic degrading bacteria isolated from landfill sites. *Int J Clin Microbiol Biochem Technol* 3(1):030–035. https://doi.org/10.29328/journal.ijcmbt.1001011

Bochalya MS, Kumar A, Rathi AS, Raj K (2016) Isolation and characterization of rhizobacteria from mustard field. *Biosci Biotechnol Res Asia* 13(4):2281–2286

Bruno WJ, Socci ND, Halpern AL (2000) Weighted neighbor joining: a likelihood-based approach to distance-based phylogeny reconstruction. *Mol Biol Evol* 17(1):189–197

Cai Z, Li M, Zhu Z, Wang X, Huang Y, Li T, Yan M (2023) Biological degradation of plastics and microplastics: a recent perspective on associated mechanisms and influencing factors. *Microorganisms* 11(7):1661. https://doi.org/10.3390/microorganisms11071661

Charnock C (2021) Norwegian soils and waters contain mesophilic, plastic-associated bacteria. *Microorganisms* 9(1):94. https://doi.org/10.3390/microorganisms9010094

Chioma O, Ogechukwu M, Bright O, Simon O, Chinyere AF (2013) Isolation and characterization of biosurfactants producing bacteria from oil polluted soil. *J Nat Sci Res* 3(5):119–123

de Fretes CE, Sohilait MR, Pesilette RN (2024) Low-density polyethylene biodegradation by the *Pantoea* sp. TR-C2 isolated from seabed sediment. *AACL Bioflux* 17(6):2735–2741

Dhali SL, Parida D, Kumar B, Bala K (2024) Recent trends in microbial and enzymatic plastic degradation: a solution for plastic pollution predicaments. *Biotechnol Sustain Mater* 1(1):11

Dubey AP, Thalla AK (2025) Bioprospecting indigenous bacteria from landfill leachate for enhanced polypropylene microplastics degradation. *J Hazard Mater* 487:137139. https://doi.org/10.1016/j.jhazmat.2025.137139

EY India (2025) The plastic circular economy in India: current dynamics and scaling vectors. Ernst & Young India Publications

Haas B, Bonifait L, Vaillancourt K, Charette SJ, Gottschalk M, Grenier D (2014) Characterization of DNase activity and gene in *Streptococcus suis* and evidence for a role as virulence factor. *BMC Res Notes* 7(1):424

Isha, Ali S, Chang YC (2024) Biodegradation of polyethylene using *Bacillus tropicus* isolated from sewage wastewater treatment plant. *Processes* 12(11):2516

Javid F, Ali G, Rehman A, Naeem R, Ali I, Naz I (2024) Assessment of plastic degradation by indigenous bacteria from waste disposal sites. *Emerg Contam* 10(3):100323

Kotova IB, Taktarova YV, Tsavkelova EA, Egorova MA, Bubnov IA, Malakhova DV, Bonch-Osmolovskaya EA (2021) Microbial degradation of plastics and approaches to make it more efficient. *Microbiology* 90(6):671–701

Lad V, Panchal D, Pithawala M, Dwivedi MK, Amaresan N (2022) Determination of hemolytic activity. In: Biosafety assessment of probiotic potential. Springer, pp 43–46

MacFaddin JF (2000) Biochemical tests for identification of medical bacteria, 3rd edn. Williams & Wilkins

Maroof L, Khan I, Yoo HS, Kim S, Park HT, Ahmad B, Azam S (2021) Identification and characterization of low-density polyethylene-degrading bacteria isolated from soils of waste disposal sites. *Environ Eng Res* 26(3):200167. https://doi.org/10.4491/eer.2020.167

Merchant M, Mande SS, Sar P (2025) Microbial community enrichment and transition in landfill for the biotransformation of unpretreated low-density polyethylene (LDPE) under aerobic and anaerobic conditions. *Chemosphere* 144429. https://doi.org/10.1016/j.chemosphere.2025.144429

NITI Aayog (2022) Alternative products and technologies to plastics and their applications. National Institution for Transforming India, Government of India

OECD (2022) Global plastics outlook: policy scenarios to 2060. OECD Publishing. https://doi.org/10.1787/aa1edf33-en

Ren SY, Ni HG (2023) Biodeterioration of microplastics by bacteria isolated from mangrove sediment. *Toxics* 11(5):432. https://doi.org/10.3390/toxics11050432

Sarker RK, Chakraborty P, Paul P, Chatterjee A, Tribedi P (2020) Degradation of low-density polyethylene (LDPE) by *Enterobacter cloacae* AKS7: a potential step towards sustainable environmental remediation. *Arch Microbiol* 202:2117–2125. https://doi.org/10.1007/s00203-020-01926-8

Sharma H, Neelam DK (2025) Biodegradation of LDPE-based vegetable packaging films through bacteria isolated from a waste disposal site. *J Pure Appl Microbiol* 19(2):1434–1447. https://doi.org/10.22207/JPAM.19.2.47

Shilpa S, Basak N, Meena SS (2024) Biodegradation of low-density polythene (LDPE) by a novel strain of *Pseudomonas aeruginosa* WD4 isolated from plastic dumpsite. *Biodegradation* 35(5):641–655. https://doi.org/10.1007/s10532-023-10061-2

Skariyachan S, Manjunatha V, Sultana S, Jois C, Bai V, Vasist KS (2016) Novel bacterial consortia isolated from plastic garbage processing areas demonstrated enhanced degradation for low density polyethylene. *Environ Sci Pollut Res* 23(18):18307–18319

Skariyachan S, Taskeen N, Kishore AP, Krishna BV, Naidu G (2021) Novel consortia of *Enterobacter* and *Pseudomonas* formulated from cow dung exhibited enhanced biodegradation of polyethylene and polypropylene. *J Environ Manage* 284:112030

Thompson RC, Swan SH, Moore CJ, vom Saal FS (2009) Our plastic age. *Philos Trans R Soc B Biol Sci* 364(1526):1973–1976

Ting ASY, Sallahudin AY (2025) Biodegradation potential of mixed cultures of *Bacillus* sp. and *Priestia* sp. from landfill investigated on low-density polyethylene (LDPE) sheets. *Water Air Soil Pollut* 236:712. https://doi.org/10.1007/s11270-025-08369-1

Tirkey A, Upadhyay LSB (2025) Introducing the LDPE degrading microbes of sedimentary systems: from dumpsite to laboratory. *Environ Sci Adv* 4:952–963. https://doi.org/10.1039/D5VA00058K

Tripathi N, Zubair M, Sapra A (2025) Gram staining. In: StatPearls. StatPearls Publishing

Uddin M, Krishnan SV, Pal SK, Vinu R, Sekar K, Ramani K (2025) Accelerating biodegradation efficiency of low-density polyethylene and its hazardous dissolved organic matter using unexplored polyolefin-respiring bacteria: new insights on degradation characterization, biomolecule influence and biotransformation pathways. *J Hazard Mater* 492:138144. https://doi.org/10.1016/j.jhazmat.2025.138144

Urbanek AK, Rymowicz W, Mirończuk AM (2018) Degradation of plastics and plastic-associated bacteria in cold marine habitats. *Appl Microbiol Biotechnol* 102(18):7669–7678

Wei R, Zimmermann W (2017) Microbial enzymes for the recycling of recalcitrant petroleum-based plastics: how far are we? *Microb Biotechnol* 10(6):1308–1322

Wilkes RA, Aristilde L (2017) Degradation and metabolism of synthetic plastics and associated products by *Pseudomonas aeruginosa*: capabilities and challenges. *J Appl Microbiol* 123(3):582–593

Yoshida S, Hiraga K, Takehana T, Taniguchi I, Yamaji H, Maeda Y, Toyohara K, Miyamoto K, Kimura Y, Oda K (2016) A bacterium that degrades and assimilates poly(ethylene terephthalate). *Science* 351(6278):1196–1199

Zhang Z, Fan X, Zhang R, Pan X, Zhang X, Ding Y, Liu Y (2025) Biodegradation characterization and mechanism of low-density polyethylene by the enriched mixed-culture from plastic-contaminated soil. *J Hazard Mater* 494:138530. https://doi.org/10.1016/j.jhazmat.2025.138530

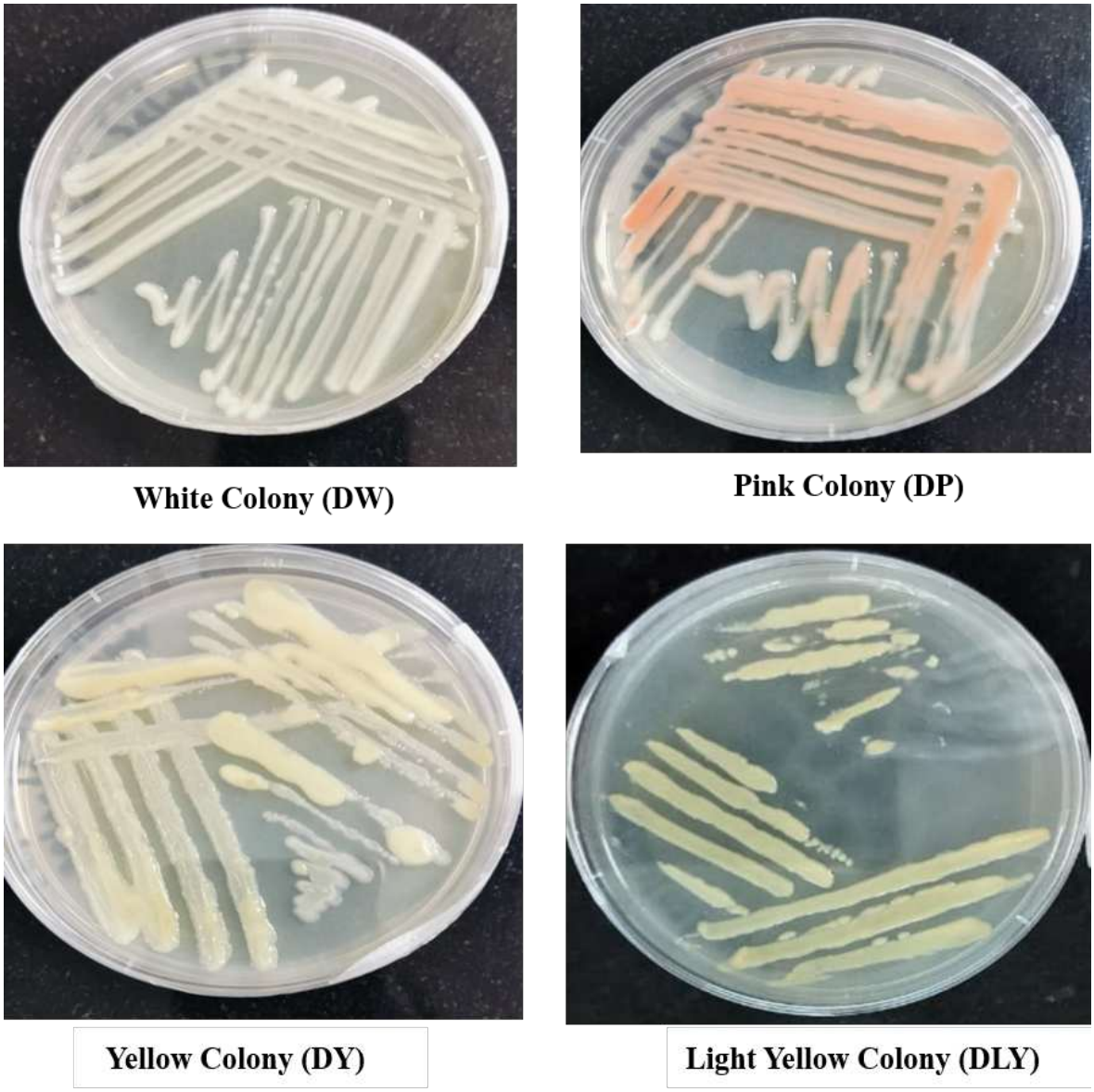


Fig. 1. Morphologically distinct bacterial isolates exhibiting white (DW), pink (DP), yellow (DY), and light-yellow (DLY) colony pigmentation, isolated from landfill soil samples and purified on Luria–Bertani (LB) agar medium.

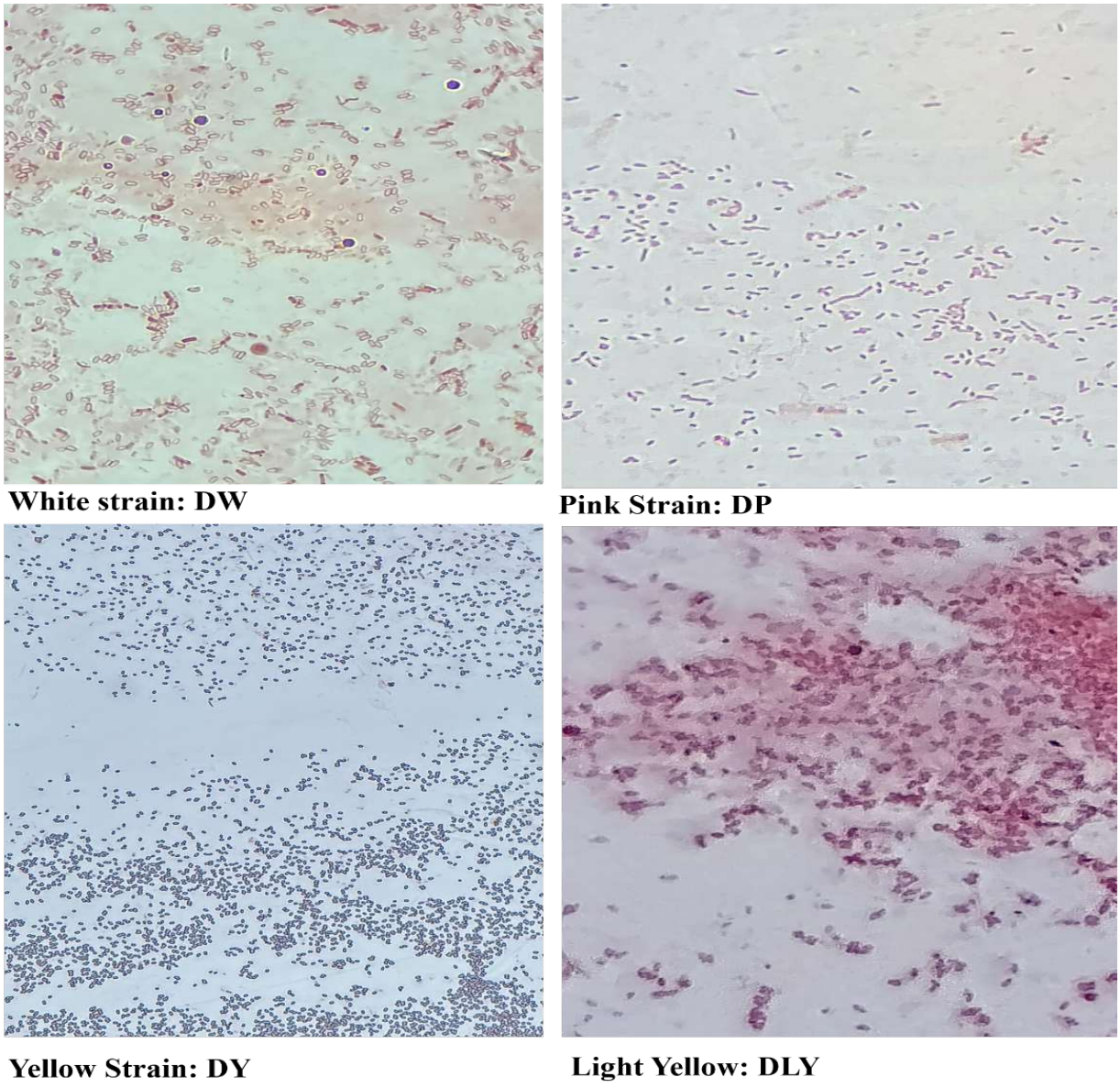


Fig. 2. Gram staining of the four purified bacterial isolates showing Gram-negative, rod-shaped morphology under oil-immersion microscopy. Microscopy was performed using a 100× oil-immersion objective (total magnification 1000×).

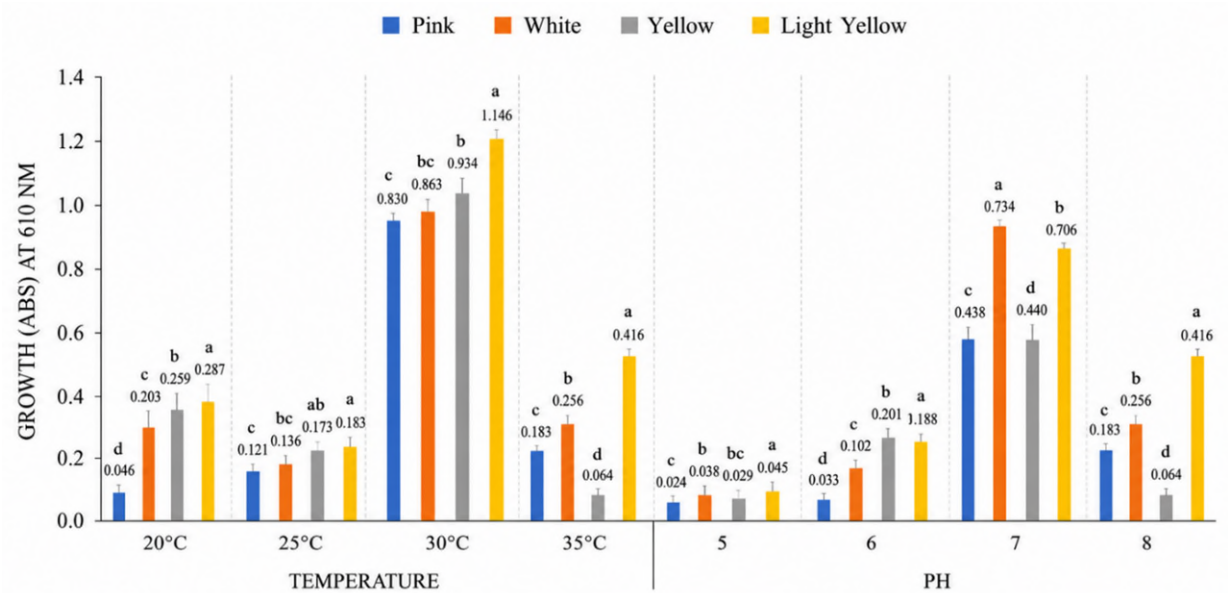


Fig. 3. Growth pattern of bacterial isolates measured as absorbance at 610 nm (OD_{610}) under different physiological conditions. (A) Effect of temperature (20, 25, 30, and 35°C). (B) Effect of pH (5, 6, 7, and 8). Bars represent mean growth values ± SE. Different lowercase letters indicate statistically significant differences among treatments according to one-way ANOVA followed by Tukey's HSD post hoc test ($P < 0.05$).

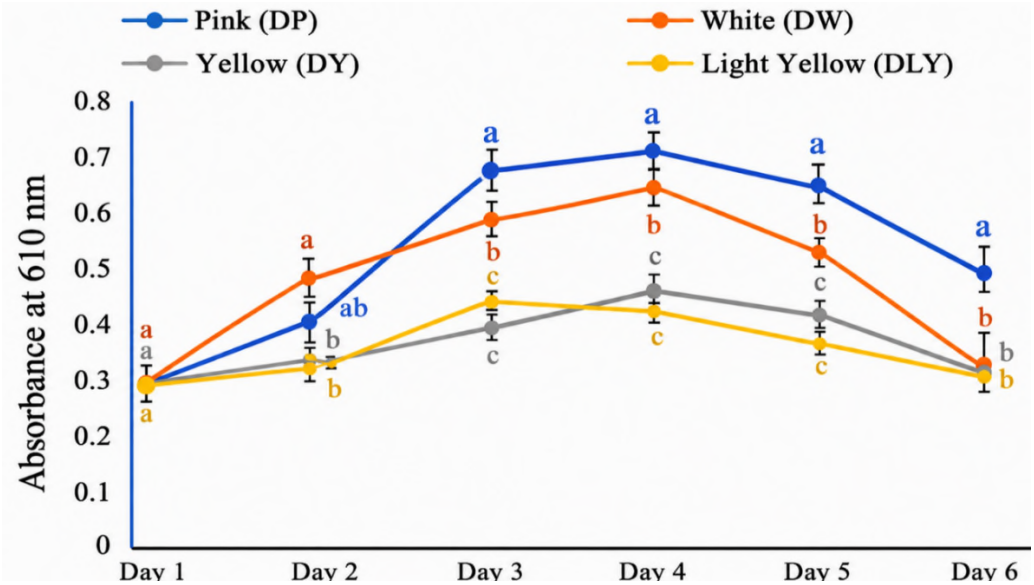


Fig. 4. Growth kinetics of bacterial strains measured as absorbance at 610 nm (OD_{610}) over six days. Values represent mean ± SE (n = 3). Distinct symbols/lines represent Pink (DP), White (DW), Yellow (DY), and Light-yellow (DLY) isolates. Statistical differences were evaluated by one-way ANOVA followed by Tukey's multiple comparison test ($P < 0.05$); significance annotations are retained only where relevant for visual clarity.

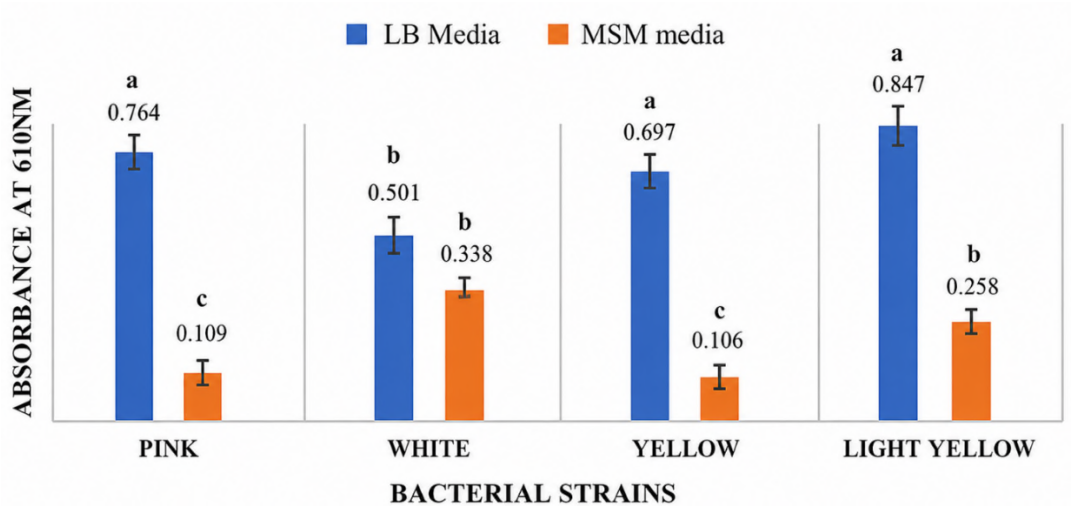


Fig. 5. Comparative growth of bacterial isolates in Luria–Bertani (LB) medium and Minimal Salt Medium (MSM), measured as absorbance at 610 nm (OD_{610}). The figure compares growth under nutrient-rich LB and nutrient-limited MSM conditions.

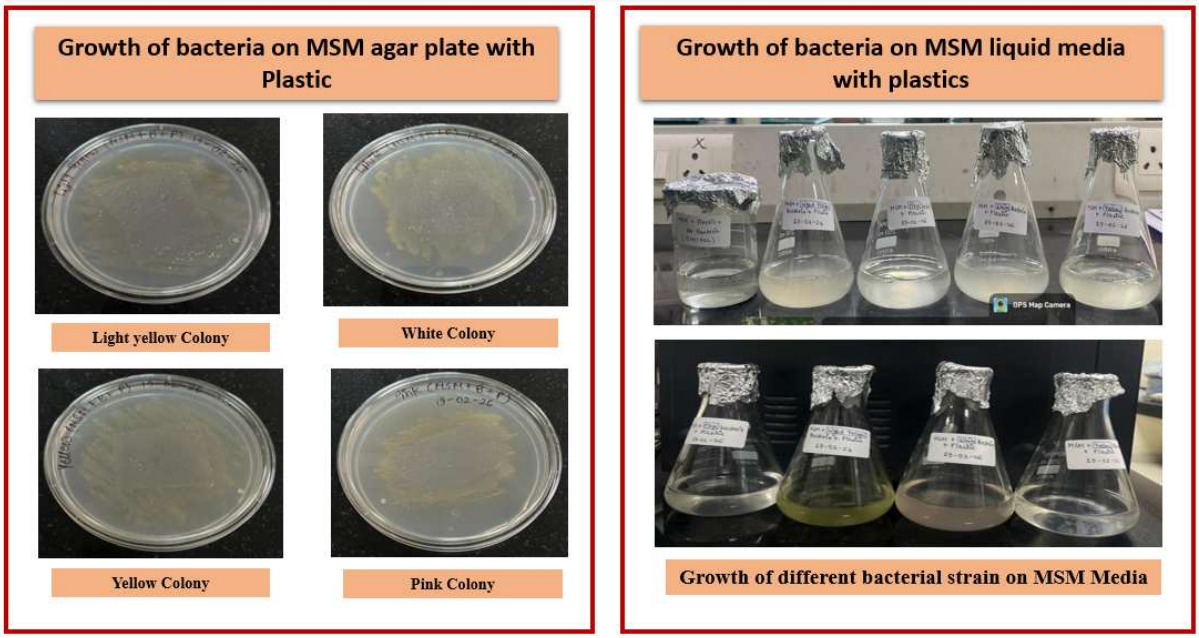
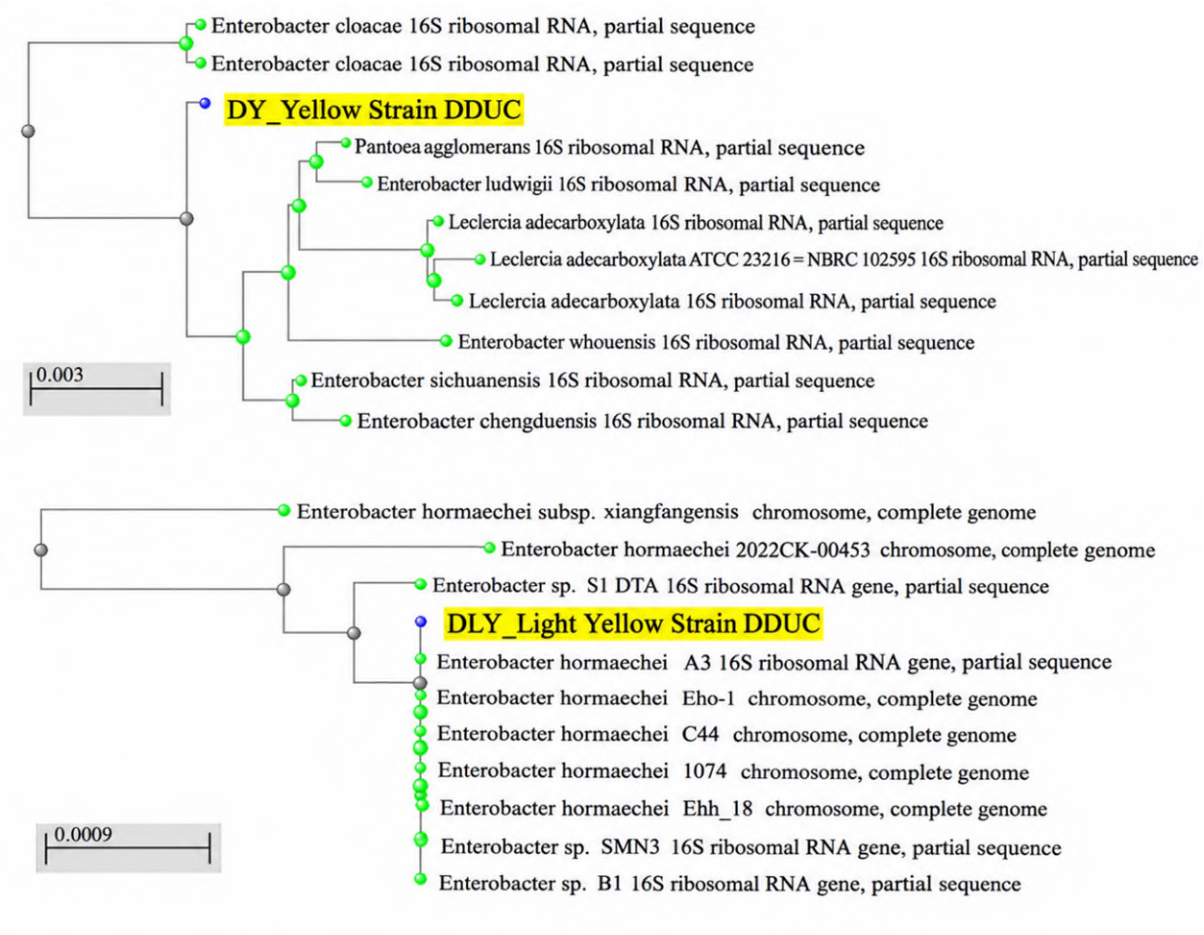


Fig. 6. Growth of bacterial isolates on Minimal Salt Medium (MSM) supplemented with plastic. **(A)** Growth on MSM agar plates showing colony development of Light-yellow (DLY), White (DW), Yellow (DY), and Pink (DP) isolates in the presence of plastic. **(B)** Growth of the different bacterial strains in MSM liquid media containing plastic substrate, showing visible turbidity differences among the four isolates relative to the uninoculated control.


Enterobacter cloacae 16S ribosomal RNA, partial sequence
Enterobacter cloacae 16S ribosomal RNA, partial sequence
DY_Yellow Strain DDUC
Pantoea agglomerans 16S ribosomal RNA, partial sequence
Enterobacter ludwigii 16S ribosomal RNA, partial sequence
Leclercia adecarboxylata 16S ribosomal RNA, partial sequence
Leclercia adecarboxylata ATCC 23216 = NBRC 102595 16S ribosomal RNA, partial sequence
Leclercia adecarboxylata 16S ribosomal RNA, partial sequence
Enterobacter whouensis 16S ribosomal RNA, partial sequence
0.003
Enterobacter sichuanensis 16S ribosomal RNA, partial sequence
Enterobacter chengduensis 16S ribosomal RNA, partial sequence
Enterobacter hormaechei subsp. xiangfangensis chromosome, complete genome
Enterobacter hormaechei 2022CK-00453 chromosome, complete genome
Enterobacter sp. S1 DTA 16S ribosomal RNA gene, partial sequence
DLY_Light Yellow Strain DDUC
Enterobacter hormaechei A3 16S ribosomal RNA gene, partial sequence
Enterobacter hormaechei Eho-1 chromosome, complete genome
Enterobacter hormaechei C44 chromosome, complete genome
Enterobacter hormaechei 1074 chromosome, complete genome
Enterobacter hormaechei Ehh_18 chromosome, complete genome
0.0009
Enterobacter sp. SMN3 16S ribosomal RNA gene, partial sequence
Enterobacter sp. B1 16S ribosomal RNA gene, partial sequence

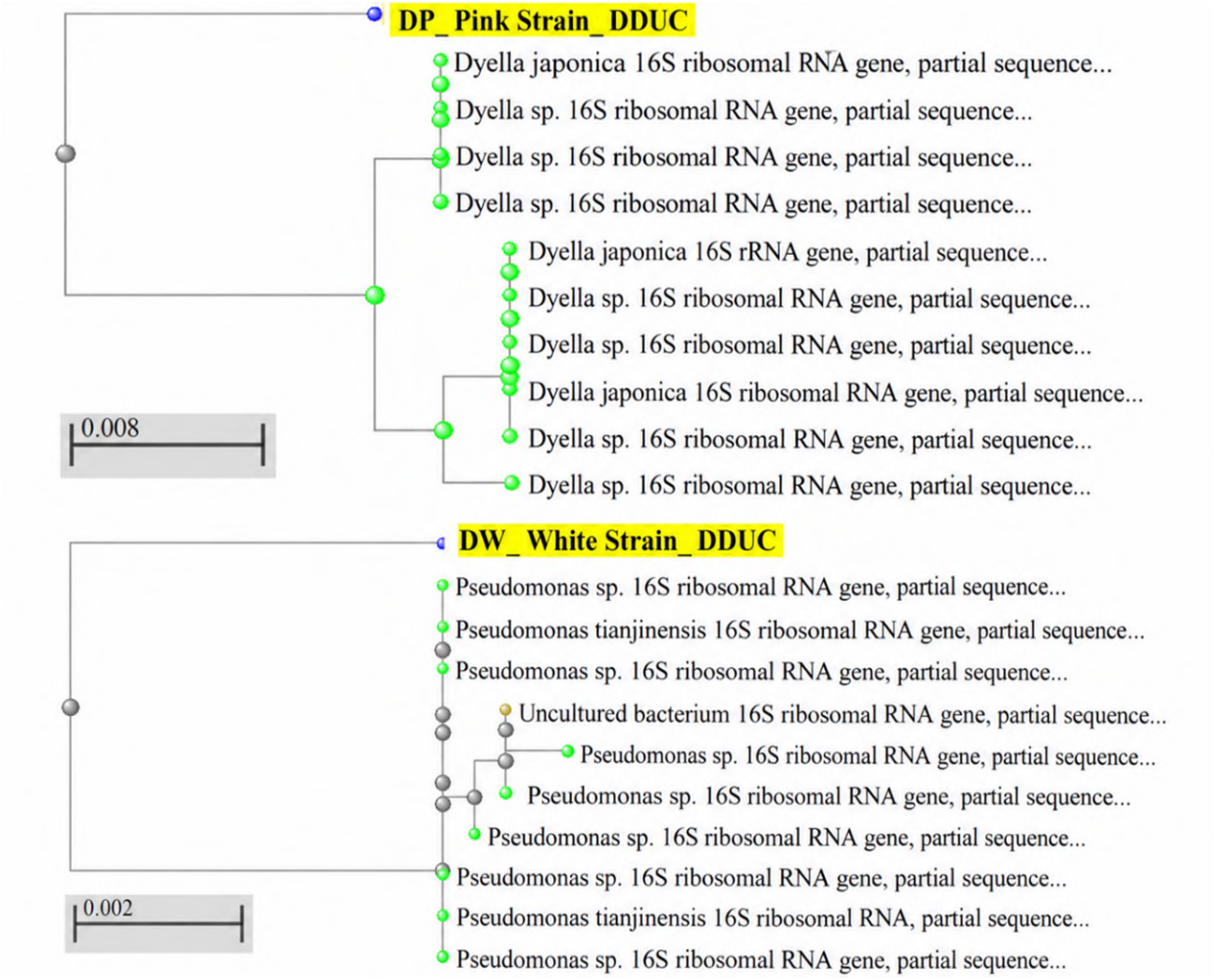


Fig. 7. Phylogenetic trees constructed using 16S rRNA gene sequences showing the evolutionary relationships of DDUC bacterial isolates with their closest relatives retrieved from the NCBI GenBank database. Bootstrap values (shown at the nodes) were obtained from 1,000 replicates. **Bootstrap value interpretation: ≥90%** = High support; **70–89%** = Moderate support; **<70%** = Low support.

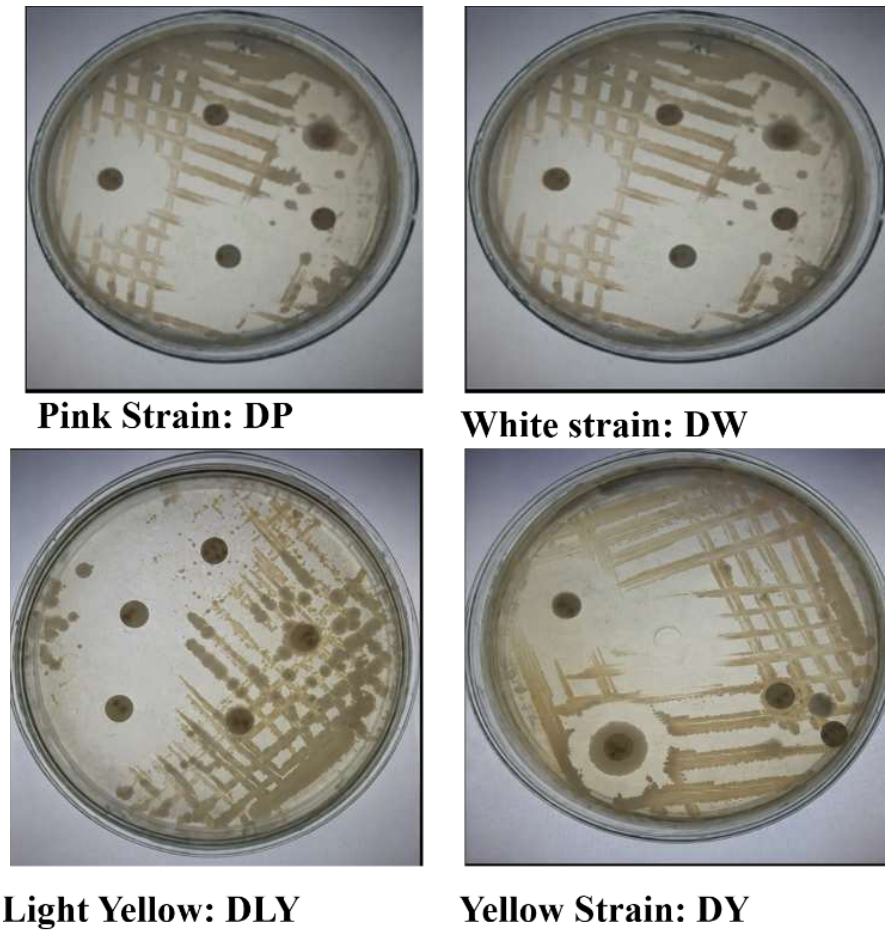


Fig. 8. Antibiotic sensitivity test on Mueller-Hinton agar showed highest susceptibility in White (DW) strain to Cefepime (20 mm) and Penicillin (18 mm), Light Yellow (DLY) Strain to Chloramphenicol (22 mm), Pink (DP) strain as multidrug-resistant (0–5 mm zones), and Yellow strain (DY) with moderate sensitivity to Neomycin (14 mm) and Streptomycin (13 mm).

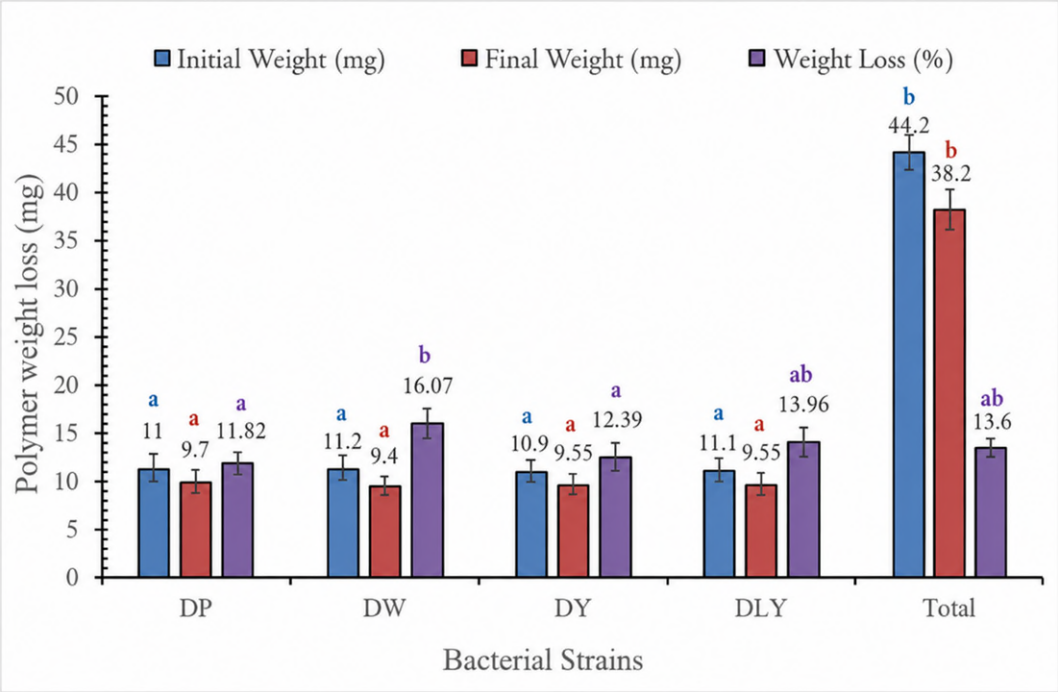


Fig. 9. Initial weight, final weight, and apparent percentage mass loss of the LDPE substrate following treatment with bacterial isolates Pink (DP), White (DW), Yellow (DY), and Light Yellow (DLY). Values are presented as mean ± SE. Different lowercase letters above bars indicate significant differences among bacterial strains according to one-way ANOVA followed by Tukey's HSD test at $P < 0.05$.

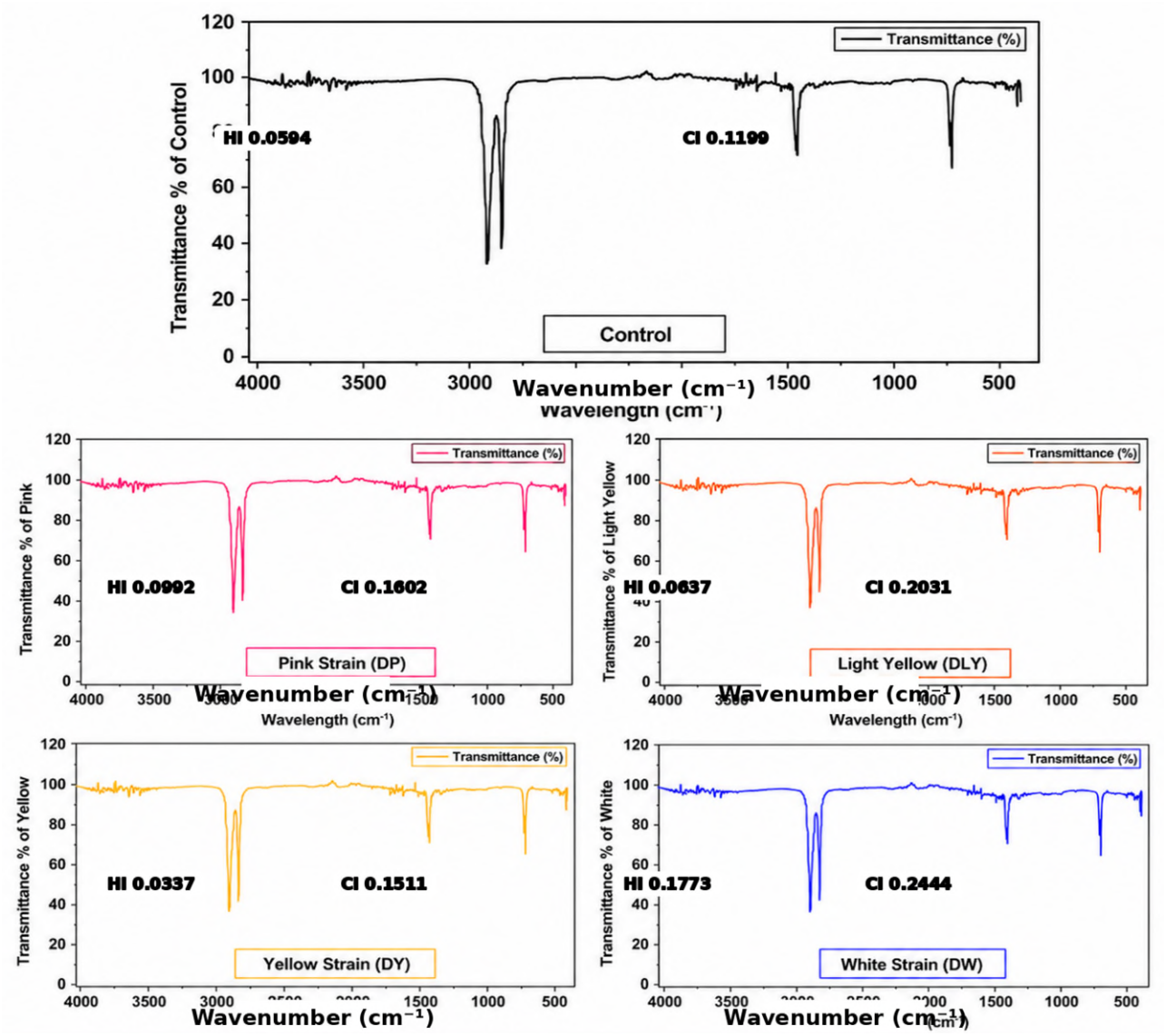


Fig. 10. FTIR spectra of untreated control and bacterial-treated LDPE films [Pink (DP), Light-yellow (DLY), Yellow (DY), and White (DW)] showing isolate-associated changes in absorption bands related to oxygen-containing functional groups. The corresponding Carbonyl Index (CI) and Hydroxyl Index (HI) values are: control, CI = 0.1199 and HI = 0.0594; DP, CI = 0.1602 and HI = 0.0992; DLY, CI = 0.2031 and HI = 0.0637; DY, CI = 0.1511 and HI = 0.0337; and DW, CI = 0.2444 and HI = 0.1773. The x-axis represents wavenumber (cm^{-1}).

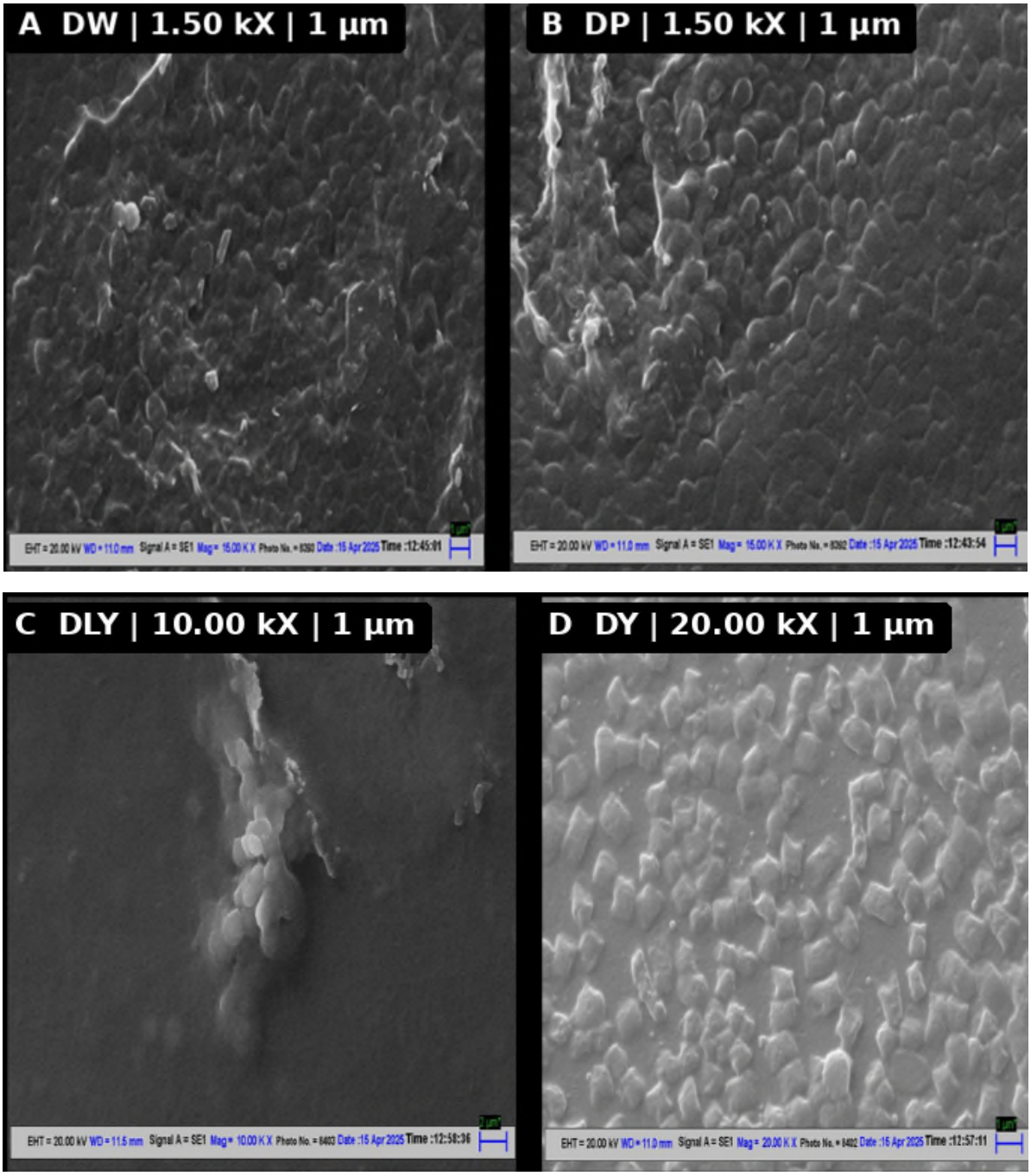


Fig. 11. Scanning electron micrographs (SEM) of bacterial isolates colonizing separate polyethylene (PE) film squares used for SEM analysis. Panels: (A) White isolate (DW), 1.50 kX; (B) Pink isolate (DP), 1.50 kX; (C) Light-yellow isolate (DLY), 10.00 kX; and (D) Yellow isolate (DY), 20.00 kX. Scale bars: 1 µm. The SEM substrate was PE film used specifically for the 7-day SEM colonization assay and was not the 45-day LDPE film used for the gravimetric LDPE gravimetric assay.

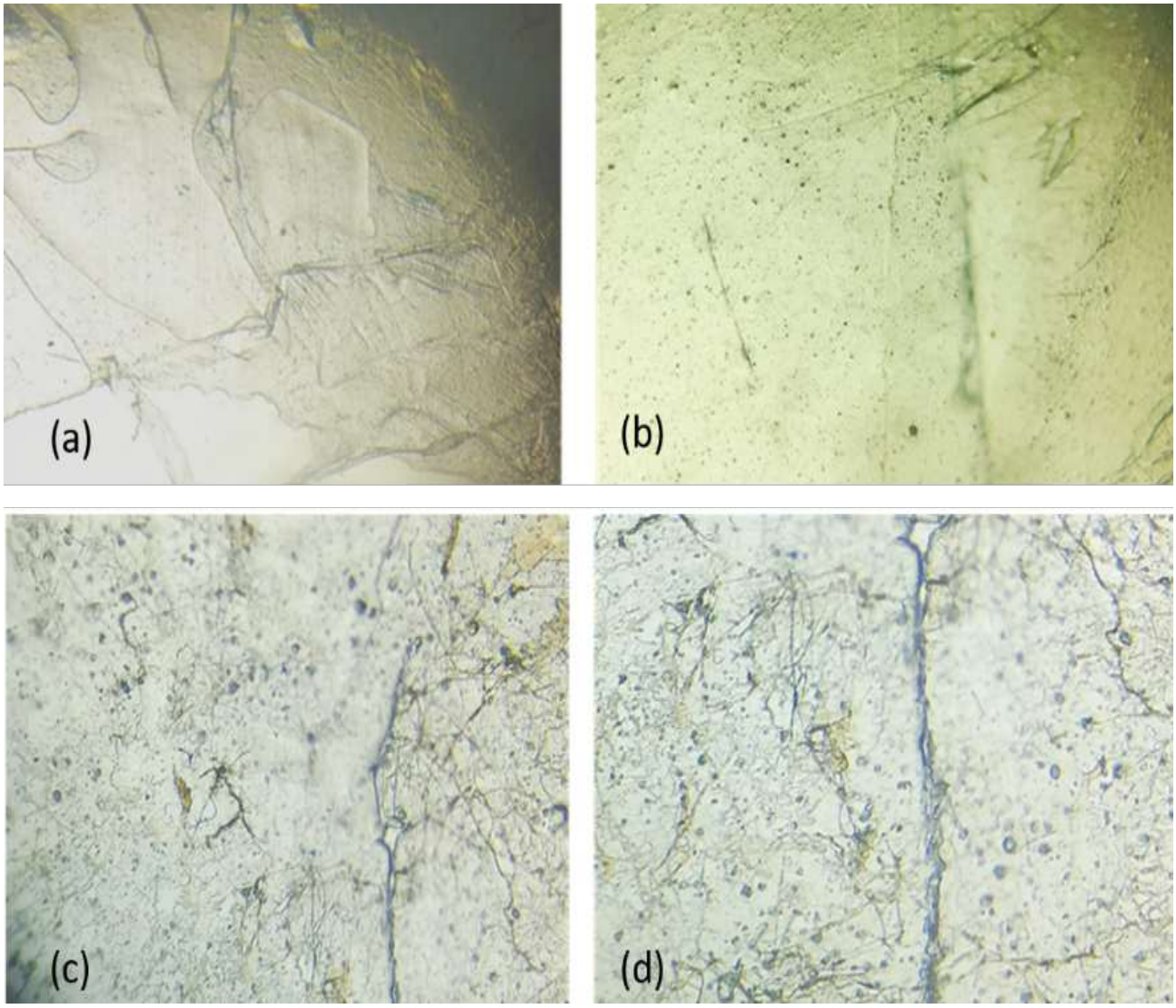


Fig. 12. Representative bright-field microscopic observations of LDPE films after 45 days of incubation. Panels: (A) White colony (DW), (B) Pink colony (DP), (C) Yellow colony (DY), and (D) Light-yellow colony (DLY), illustrating representative surface morphological alterations, including roughening and irregularities where visible. The LDPE transformation experiment comprised three independent biological replicates; the images shown are representative fields.

Table 1. Summary of the closest BLASTn matches of the 16S rRNA gene sequences of DDUC bacterial isolates, showing the nearest taxonomic affiliations, percentage sequence identity, and confidence level of species identification based on sequence similarity.

Isolate	Closest BLAST match(es)	% Identity Range*	Confidence
White Strain (DW)	*Pseudomonas* sp.	99.2–99.8%	High
Pink Strain (DP)	*Dyella Japonica*	99.1–99.8%	High
Light Yellow (DLY)	*Enterobacter hormaechei*	99.0–99.7%	High
Yellow Strain (DY)	*Pantoea agglomerans*	98.5–99.3%	High

Confidence levels were assigned based on sequence similarity and phylogenetic clustering, where ≥99% identity indicates high confidence in species-level assignment.

Table 2. Environmental Characterization of Four Bacterial Isolates Based on Growth Under Different Physicochemical Conditions

Biochemical Test	DW (*Pseudomonas aeruginosa*)	DP (*Dyella japonica*)	DLY (*Enterobacter* sp. strain S1 DTA)	DY (*Pantoea agglomerans*)
Indole Test	-	-	-	-
Methyl Red Test	+	+	-	+
Voges Proskauer Test	-	-	-	-
Citrate Test	+	+	+	+
Blood Agar Test	-	-	-	-
DNase Agar Test	-	-	-	-

(-) = Negative response, (+) = Positive response

Table 3. Comparative Analysis of Biochemical Traits and Extracellular Enzyme Activities of Bacterial Isolates Cultivated in LB and MSM Media

Biochemical Test	**DW**	**DP**	**DY**	**DLY**	**DW**	**DP**	**DY**	**DLY**
	(Grown in LB Medium)				**(Grown in MSM Medium)**			
Catalase Test	++	++	++	++	+	+	+	+
Cellulase Test	++	-	-	++	+	-	-	++
Alpha Amylase Test	++	-	++	-	+	-	+	-
Protease Test	++	-	++	-	++	-	++	-
Lipase/ Esterase Test	-	-	-	-	++	-	-	-

Table 4. FTIR-based assessment of carbonyl index (CI), hydroxyl index (HI), and structural modifications in LDPE films following bacterial treatment.

Sample	CI	HI	Inference
Control (c)	0.1199	0.0594	Baseline plastic; no oxidation.
White (DW)	**0.2444**	**0.1773**	Highest oxidation; most effective.
Light Yellow (DLY)	0.2031	0.0637	Moderate oxidation & chain scission.
Pink (DP)	0.1602	0.0992	Early surface modification.
Yellow (DY)	0.1511	0.0337	Minimal interaction; mostly stable.

Supplementary Files

This is a list of supplementary files associated with this preprint. Click to download.

- SplimentoryData.pptx